

**Shear thinning silicone-PEG block  
copolymers**

By: Abidur Rahman, BHSc

A Thesis

Submitted to the School of Graduate Studies in Partial Fulfilment  
of the Requirements for the Degree  
Master of Science

McMaster University

© Copyright by Abidur Rahman, January 2015

MASTER OF SCIENCE

McMaster University

Hamilton, ON

Title: Shear thinning silicone-PEG block copolymers

AUTHOR

Abidur Rahman

Hons. BHSc (McMaster University)

SUPERVISORS

Dr. Michael A. Brook

COMMITTEE MEMBERS Dr. Todd Hoare

NUMBER OF PAGES

xii, 91

## **ABSTRACT**

In this work, we created shear thinning block copolymers that could be potentially utilized as an artificial vitreous replacement. The materials were created using poly(ethylene glycol) (PEG) and silicone polymers, respectively, due to their high biocompatibility. Both the ABA and BAB geometry triblock copolymers were created and were characterized using parallel plate and cone-and plate rheometers. It was observed that the materials from both geometries exhibited a decrease in viscosity with increasing shear rates, thus fulfilling the criteria of being a shear thinning material.

The materials were also characterized under different aqueous conditions. It was observed that the materials with a higher PEG composition were better able to retain their physical structure – did not disperse into aqueous solutions – at higher water content levels. The materials that retained their structure were also shown to retain their shear thinning properties.

In the absence of solvent, the opacity of the materials increased with increasing PEG composition ratio per copolymer chain. When exposed to different aqueous conditions, the opacity of the materials was found to decrease at specific water concentrations. Materials with larger PEG blocks required a greater water content to exhibit optimal light transmission.

## **ACKNOWLEDGEMENTS**

I would like to express my utmost gratitude to my supervisor Dr. Michael A. Brook for being an amazing mentor, facilitator, and educator throughout my graduate education. Learning from him was truly a privilege as he inspired me to continuously push myself to be better. I would also like to thank my committee supervisor, Dr. Todd Hoare, for helping me understand difficult topics and taking time out of his busy schedule to answer any question I had throughout my graduate career.

I could not have accomplished my work without the continuous help and support from the past and present Brook group members and the departmental staff. I would specially like to thank, John Grande, Vinodh Rajendra, Amanda Fawcett, Jason Zhang, Dan Chen, Madiha Khan, Virginie Delhorbe, Anna Szelag, Laura Dodge, Hanjiang Dong, Talena Rambarran, Marlena Whinton, Alyssa Schneider, Ayodele Fatona, Jenn Morgan, Tomas Urlich, Nora Labbancz, Kay Chen, Kelvin Li, Tara Dickie, Michael Coulson, Jeff Suen, Tony Chen, Adam Kowalczyk, Linda Li, Roozbeh Mafi, and Elizabeth Takacs. I would also like to thank Jack Huang, Tarak Ahmed, Amzad Khan, Anne Xia, Mark Tenn, Lynn Yuan, Celisse Bibr, Max Goodwin, Chris White, Andrew Soave, Jenna Webber, Jasmine Chahal, Kristy Yiu, Aarti Sayal, Ioana Stoichituiu, Vishu Karthik, Hrishu Suresh, Jeff Mah, and Adeel Akhtar for keeping me sane and nourished throughout this process. I would also like to thank my professor Stash Nastos for the continuous encouragement and acting as like an older brother throughout my entire university career.

Of all the people in this world, I would most like to thank my mother, Mansura Begum, my Father Mohammad Sanaullah, and my brothers Azizur and Anisur Rahman

for being there for me at all times and helping me overcome every obstacle placed in my way. Without you, I would be nothing and I owe everything I have achieved to you.

# TABLE OF CONTENTS

## Chapter 1: Background and Scope of Project

1-1	Introduction	1
1-2	Vitreous	3
1-2.1	Criteria for an Ideal Vitreous Substitute	4
1-2.2	Previous Vitreous Replacements	4
1-2.2.1	Natural Materials	5
1-2.2.2	Semi-Synthetic Polymers	5
1-2.2.3	Synthetic Polymers	6
1-3	Rheology	7
1-3.1	Complex and Shear Viscosity	8
1-3.2	Newtonian and Non-Newtonian Fluids	9
1-4	Shear thinning materials	10
1-5	Measurement Techniques	11
1-6	Proposed preparation of shear thinning PEG-PDMS copolymers	12
1-6.1	Silicones and their biocompatibility	12
1-6.2	Silicone oil retinal tamponade	12
1-6.3	Silicone oil preparation	14
1-6.4	Hydrosilylation	15
1-7	Methods to Improve Hydrophilicity	16
1-7.1	Poly(ethylene glycol)	17
1-8	Block copolymers morphologies	18
1-9	Scope of Projects	20
1-10	References	22

## Chapter 2: Characterization of PEG-PDMS block copolymers of ABA and BAB geometry

2-1	Introduction	27
2-2	Materials and Methods	31
2-2.1	Materials	31
2-2.2	Synthesis of Allylated PEG	33
2-2.3	Linear ABA and BAB block copolymer synthesis	34
2-2.4	<sup>b</sup> BA <sup>b</sup> B block copolymer synthesis	35
2-2.5	Characterization of the samples	37
2-2.5.1	Rheology	37
2-2.5.2	Turbidity measurement	37
2-3	Results	38
2-3.1	Complex viscosity measurements	38
2-3.2	Shear viscosity measurements	39

	2-3.2.1	Rheology of linear ABA block copolymers	40
	2-3.2.2	Rheology of linear BAB block copolymers	41
	2-3.2.3	Rheology of <sup>b</sup> BA <sup>b</sup> B block copolymers	42
2-3.3		Turbidity Measurements	44
	2-3.3.1	Linear ABA block copolymers	44
	2-3.3.2	Linear BAB block copolymers	44
2-4		Discussion	45
	2-4.1	Effect of PEG molecular weight on the copolymer viscosity	45
	2-4.2	Effect of PEG molecular weight and copolymer geometry on viscosity	49
	2-4.3	Comparing <sup>b</sup> BA <sup>b</sup> B copolymers with linear BAB copolymers with 850 g/mol PDMS chain	50
	2-4.4	Effect of PEG block size on light transmission of copolymers	51
2-5		Conclusion	53
2-6		Acknowledgements	54
2-7		References	55

### **Chapter 3: Characterization of hydrated PEG-PDMS block copolymers of ABA and BAB geometry**

3-1		Introduction	58
3-2		Experimental section	60
	3-2.1	Materials	60
	3-2.2	Sample Creation: Hydration of Copolymers	61
	3-2.3	Characterization of the samples	62
		3-2.3.1 Rheology	62
		3-2.3.2 Turbidity measurements	62
		3-2.3.3 Refractive index measurements	62
3-3		Results	63
	3-3.1	Shear Viscosity Measurements	63
	3-3.2	Turbidity Measurements	67
		3-3.2.1 ABA Block Copolymers	67
		3-3.2.2 BAB Block Copolymers	68
	3-3.3	Refractive Index for the Hydrated Copolymers	69
3-4		Discussion	71
	3-4.1	Shear Viscosity of the Linear Hydrated Copolymers	71
	3-4.2	Effect of PEG and PDMS composition per copolymer chain and molecular weight on the structural integrity	76
	3-4.3	Effect of PEG block size on light transmission of hydrated copolymers	77
	3-4.4	Comparison of copolymers with past materials	79
	3-4.5	Possible modifications to create an optimal retinal tamponade	80
3-5		Conclusion	83
3-6		Acknowledgements	83
3-7		References	84

## Appendix A:

A-1	Chemical Structures and H-NMR of Allylated PEG	86
A-1.1	Monoallylated PEG	86
A-1.2	Diallylated PEG	86
A-2	Chemical Structures and H-NMR of Linear ABA and BAB Block Copolymers	87
A-2.1	Linear ABA Block copolymers	87
A-2.2	Linear BAB Block copolymers	88
A-3	Chemical Structures and H-NMR of Branched Pendant Group <sup>b</sup> BA <sup>b</sup> B Block Copolymers	90



# LIST OF FIGURES

## Chapter 1: Background and Scope of Project

Figure 1-1	Image of a human vitreous.	3
Figure 1-2	Shear viscosity profiles of plastic and pseudoplastic-shear thinning materials.	10
Figure 1-3	Schematic representations of the different geometries (from left to right: parallel plate, cone and plate, and concentric cylinders) of the rheometers utilized for rheological testing.	12
Figure 1-4	Schematic representation hydride terminated PDMS synthesis followed by end group modification.	15
Figure 1-5	Generalized transition metal catalyzed hydrosilylation reaction mechanism.	16
Figure 1-6	Ring opening anionic polymerization scheme to create PEG followed by end group modification (B- is EtMgBr).	18
Figure 1-7	Block copolymer morphologies of copolymers containing two types of blocks.	19

## Chapter 2: Characterization of PEG-PDMS block copolymers of ABA and BAB geometry

Figure 2-1	Schematic diagram of the human eye.	27
Figure 2-2	Schematic diagrams of rest state (left) and sheared state (right) of shear thinning copolymers.	30
Figure 2-3	Schematic diagrams of Karstedt's catalyst (left) and Wilkinson's catalyst (right).	32
Figure 2-4	Reaction schemes for linear pendant group ABA (top left), linear pendant group BAB (top right), and branched pendant BAB (bottom) block copolymers.	36
Figure 2-5	Strain sweep test data (top row) and frequency sweep test (bottom row) from left to right: ABA PEG 750 – PDMS 17000, ABA PEG 750 – PDMS 28000, ABA PEG 2000 – PDMS 17000, ABA PEG 2000 – PDMS 28000.	39

Figure 2-6	Shear sweep tests A) ABA PEG 350 – PDMS 17000 B) ABA PEG 750 – PDMS 17000 C) ABA PEG 2000 – PDMS 17000 D) ABA PEG 350 – PDMS 28000 E) ABA PEG 750 – PDMS 28000 F) ABA PEG 2000 – PDMS 28000 G) BAB PEG 400 – PDMS 850 H) BAB PEG 1000 – PDMS 850 I) BAB PEG 2000 – PDMS 850 J) BAB PEG 400 – PDMS 4750 K) BAB PEG 1000 – PDMS 4750 L) BAB PEG 2000 – PDMS 4750 M) <sup>b</sup> BA <sup>b</sup> B PEG 400 – PDMS 692 N) <sup>b</sup> BA <sup>b</sup> B PEG 1000 – PDMS 692 O) <sup>b</sup> BA <sup>b</sup> B PEG 2000 – PDMS 692 .	43
Figure 2-7	Turbidity data for linear ABA (left) and linear BAB (right) copolymers that allowed light transmission.	45
Figure 2-8	A) Associations of ABA copolymers as the PEG molecular weights are increased; B) Associations of BAB copolymers as the PEG molecular weights are increased; C) Association of the ordered pendant groups of the <sup>b</sup> BA <sup>b</sup> B copolymers; G) Change order of association between the blocks copolymers under the rest state (left) and sheared state (right).	48
Figure 2-9	Low shear viscosities of ABA, BAB, <sup>b</sup> BAbB block copolymers.	50

**Chapter 3: Characterization of hydrated PEG-PDMS block copolymers of ABA and BAB geometry**

Figure 3-1	Schematic diagrams of PEG forming hydrogen bonds with water molecules.	59
Figure 3-2	Schematic diagram of Karstedt's catalyst	60
Figure 3-3	Shear sweep tests, row 1: ABA PEG 350–PDMS 17000 (left), ABA PEG 350–PDMS 28000 (right); row 2: ABA PEG 750–PDMS 17000 (left), ABA PEG 750–PDMS 28000 (right); row 3: BAB PEG 400–PDMS 850 (left), BAB PEG 400–PDMS 4750 (right); row 4: BAB PEG 1000–PDMS 850 (left), BAB PEG 1000–PDMS 4750 (right).	66
Figure 3-4	Turbidity data row 1: ABA PEG 350–PDMS 17000 (left), ABA PEG 750–PDMS 17000 (middle), ABA PEG 2000–PDMS 17000 (right); row 2: ABA PEG 350–PDMS 28000 (left), ABA PEG 750–PDMS 28000 (middle), ABA PEG 2000–PDMS 28000 (right); row 3: BAB 400–PDMS 850 (left), BAB PEG 1000–PDMS 850 (middle), BAB PEG 2000–PDMS 850 (right); BAB PEG 400–PDMS 4750 (left), BAB PEG 1000–PDMS 4750 (middle), BAB PEG 2000–PDMS 4750 (right).	69

Figure 3-5	Refractive indices of PEG at various hydration levels.	71
Figure 3-6	Effect of water content level on the PEG-PEG association of the block copolymers (left); differences in association between the neat copolymers (top) and hydrated copolymers (bottom).	73
Figure 3-7	Infinite shear viscosities for the copolymers plotted against H <sub>2</sub> O:PEG ratio, row 1: ABA PEG 350–PDMS 17000 (left), ABA PEG 350–PDMS 28000 (middle), ABA PEG 750–PDMS 17000 (right); row 2: BAB PEG 400–PDMS 850 (left), BAB PEG 400–PDMS 4750 (middle), BAB PEG 1000–PDMS 850 (right); Enlarged picture of the data point with error which are in the 10 <sup>-3</sup> scale (right).	75
Figure 3-8	Effect of hydration on the refractive index of PEG.	79

## LIST OF TABLES

### Chapter 2: Characterization of PEG-PDMS block copolymers of ABA and BAB geometry

Table 2-1	Formulation of mono- and di-allylated PEG's of various molecular weights.	33
Table 2-2	Formulations of ABA and BAB block copolymers.	34
Table 2-3	Formulations of <sup>b</sup> BA <sup>b</sup> B block copolymers	35
Table 2-4	PEG and PDMS composition ratios for each of the block copolymer chains.	36

### Chapter 3: Characterization of hydrated PEG-PDMS block copolymers of ABA and BAB geometry

Table 3-1	Formulation of hydrated ABA and BAB copolymer samples.	61
Table 3-2	Refractive index measurements of hydrated copolymers that exhibited high light transmission	70

# **Background and Scope of Project**

## **1-1: Introduction**

The human eye is separated into three chambers: the anterior chamber, the posterior chamber, and the vitreous chamber.<sup>1</sup> The vitreous chamber of the eye contains a viscous fluid known as the vitreous.<sup>1</sup> Over time, the vitreous composition changes because of variations in the collagen and hyaluronic acid (HA) concentrations.<sup>2</sup> Due to these changes, the vitreous tends to lose its gel structure, shrink in size, and become more fluid.<sup>2</sup> The liquefaction process correlates with the age of the individual.<sup>3</sup> Based on a human post mortem study, it was determined that the vitreous is approximately 20% liquid by the time the eye reaches the adult size (age 14 to 18 years) and more than 50% of it is liquid between ages 80 and 90 years.<sup>3,4</sup> The shrinking of the vitreous can lead the gel to pull on the retina due to vitreoretinal traction, thus distorting vision.<sup>3</sup> This process can also lead to posterior vitreal detachment, a process where the vitreous itself pulls away from the retina and collapses into the central hollow portion of the eye.<sup>5</sup> By doing so, the vitreous tend to pull on the retina itself, thus increasing the risk of retinal detachment and retinal tears.<sup>5</sup>

Retinal detachment is characterized by the separation of retina from the subsequent vascular layer (choroid).<sup>6</sup> The separation could lead to blindness, since the retina becomes starved of nutrients and oxygen as the cells are no longer receiving nourishment from the blood.<sup>6</sup> The incidence of retinal detachment in a developed country (United Kingdom) is roughly 6.3 to 17.9 in one hundred thousand per year, with higher rates in the elderly population.<sup>6</sup> Although there are several techniques currently

available to treat these ailments, they fall far short of being optimal and thus new technology is required to improve the effectiveness of the therapeutic procedures.

To deal with the complications that arise with the ageing vitreous, a vitrectomy is commonly performed to remove the vitreous in patients who exhibit vision problems. Vitrectomies are also performed if the patient is suffering from other vitreal pathologies such as vitreous opacities and vitreal haemorrhage.<sup>7</sup> Patients undergoing vitreoretinal surgeries for retinal pathologies such as retinal detachment, age-related macular degeneration, and diabetic retinopathy would also have their vitreous removed.<sup>7</sup>

To replace the vitreous, a temporary substitute can be placed in the posterior chamber that aids in the healing process after suffering from retinal and vitreal pathologies. The primary purpose of both long and short term artificial vitreous is to achieve a tamponade effect.<sup>7</sup> Many natural and artificial substitutes have been tested and used for this purpose, such as, animal and human vitreous, gases, semi-synthetic polymers, and synthetic polymers.<sup>7,8</sup>

Gases such as perfluorocarbons and SF<sub>6</sub> (sulfur hexafluoride) are used as short term replacements for the vitreous.<sup>7,8</sup> These gases are readily able to fill the vitreous cavity, however, they have been associated with lens opacification, increased intraocular pressure, and they cause histopathological changes to the tissues surrounding the vitreous.<sup>7</sup> For longer recovery processes, silicone oils are used as retinal tamponades.<sup>7</sup> Although silicones oils are very well tolerated by the body, they fall far short of being a perfect retinal tamponade as they tend to increase the risk of glaucoma.<sup>9</sup>

To create an alternate vitreous substitute requires a thorough understanding of the materials that have previously been tested so that one can understand their benefits and shortcomings. This thesis will focus on the creation of a silicone-based long term

retinal tamponades that, hopefully, could act as a perfect substitute for the vitreous body while mitigating the risks associated with its previous counterparts.

## **1-2: Vitreous**

To understand this goal, it is first necessary to understand the structure of the vitreous which will help guide the path to creating a suitable replacement. The vitreous is mostly composed of water (~97-99%), however, it also contains collagen and hyaluronic acid amongst other proteins, glycosaminoglycans, metabolites, and other cells.<sup>7,10,11</sup> The functions of the vitreous include providing structural support for the eye, acting as a shock absorber, holding the neural and pigmented layers of the retina together, facilitating the circulation of metabolic solutes and nutrients throughout the posterior chamber, and contributing to the magnifying power of the eye.<sup>7,11</sup>

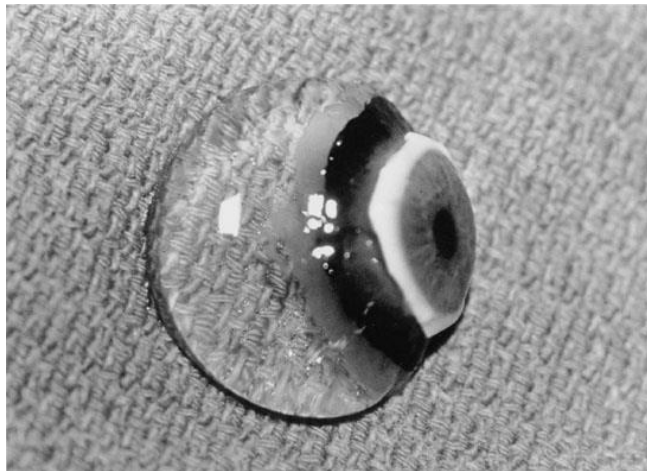


*Fig 1-1.* Image of a human vitreous (reproduced with permission)<sup>12</sup>

The vitreous attains its gel-like structure due to the collagen fibres, bound together by the proteoglycans, which form an ordered network of parallel fibrils.<sup>7,11</sup> The glycosaminoglycan chains of the proteoglycans are able to interact with the hyaluronic acid viscoelastic matrix via non-covalent bonding interactions.<sup>11</sup> The composition of the vitreous is not homogeneous.<sup>7</sup> The anterior portion of the vitreous near the lens has a 2

to 1 ratio of hyaluronic acid to collagen, while the center of the vitreous has a 10 to 1 ratio, and the edges near the retina have a ratio of approximately 20 to 1.<sup>7</sup>

### **1-2.1: Criteria for an Ideal Vitreous Substitute**

Based on the characteristics of the natural vitreous, there are several criteria that must be satisfied by an artificial vitreous substitute for it to perform its required duties.<sup>7,8,10</sup>

1. The material should be transparent, colourless, and it should not lose its transparency after it has been inserted into the posterior chamber.
2. The density and refractive index of the material should be as close as possible to that of the natural vitreous, which are approximately 1 g/cm<sup>3</sup> and 1.33, respectively.
3. The material should be non-toxic and inert under physiological conditions, both chemically and biologically, to avoid any undesirable effects.
4. The material has to be biocompatible with the surrounding tissues and should not interfere in their functions.
5. The material should not adsorb to cell surfaces or be biodegradable to increase its ability to stay in the vitreous chamber as long as possible.
6. It should be sufficiently rigid to act as an effective tamponade.
7. It should have high surface tension to avoid vitreoretinal traction (vitreous pulling on the retina).
8. The material must allow the movement of metabolites and proteins throughout the posterior chamber.
9. It should preferably be hydrophilic, while being insoluble in water.
10. It should also be injectable through a small gauge needle while retaining all of the above-mentioned properties.
11. It should be storable and sterilizable without losing any of the properties mentioned above.

### **1-2.2: Previous Vitreous Replacements**

Although there are a few treatments available which are widely used to treat vitreal and retinal pathologies, there were countless others that were tested previously, including natural materials, semi-synthetic polymers, and synthetic polymers.



### *1-2.2.1: Natural Materials*

At the beginning of the 20<sup>th</sup> Century, research was conducted where the human vitreous was replaced with rabbit, bovine, and human donor vitreous.<sup>8,13,14</sup> Physiological solutions that make up the vitreous were also utilized as possible replacements: there were no significant differences observed between the usage of these different substitutes.<sup>8,13,14</sup> Although these materials were effective in treating retinal detachment, they were not suitable as long term replacements. These treatment procedures led to various ocular problems including inflammation of the surrounding tissue, development of cataract, corneal damage, and glaucoma.<sup>8,14</sup> These shortcomings prevented the usage of these materials for prolonged periods in the posterior chamber. The shorter time periods were not sufficient to allow the retina to flatten and completely re-anneal itself to the vascular and pigmented epithelium layers making these materials ineffective retinal tamponades.

### *1-2.2.2: Semi-synthetic Polymers*

The research progressively continued towards creating alternative substitutes, which manipulated natural polymers to act as possible vitreous substitutes. The first semisynthetic polymer used for this purpose was proteolytic enzyme (proctase) treated collagen.<sup>8</sup> Upon injection of this material in human subjects, retinal reattachment was observed in some patients, however, the material caused mild inflammation and it slowly became opaque leading to blurry vision.<sup>8</sup> The material also fragmented during the injection process leading to loss of its mechanical properties.<sup>8</sup> Further testing was done with modified collagen to mitigate the inflammation, however, a successful tamponade was not achieved using collagen.<sup>7,8,13,14</sup>

Vitreous replacements were also performed using modified gelatin on humans and rabbits, with sodium hyaluronidate in humans, sodium hyaluronidate in conjunction with collagen in humans, various polysaccharide solutions in rabbits and humans, and gellan gum in conjunction with hyaluronic acid in *in-vitro* testing.<sup>7,8,13,14</sup> Although these materials showed great promise, they all fell short of their goal. These materials usually displayed short retention time in the vitreous, exhibited immune responses with the surrounding tissues leading to inflammation, and general opacification of the vitreous after the materials were injected.<sup>7,8,13,14</sup> The biggest drawbacks to these materials included bioabsorption and biodegradation *in vivo* and loss of structure and mechanical properties post-injection.<sup>7,8,13,14</sup> These problems led to further research where synthetic polymers were tested as a possible replacement to the human vitreous.

### *1-2.2.3: Synthetic Polymers*

Given that semi-synthetic materials were unable to mimic the natural vitreous, synthetic polymer research was conducted on creating materials that focus on duplicating the functional properties of the natural vitreous rather than the structural ones. The first synthetic polymer tested to act as a vitreous substitute was poly(1-vinyl-2-pyrrolidone) (PVP).<sup>8,14</sup> Different samples of diluted PVP were injected into the rabbit and human eyes to test their efficacy.<sup>8,14</sup> Although the material exhibited good biocompatibility and lower inflammatory responses than the alternatives described above, the material still had a short retention time in the vitreous and displayed opacification post injection.<sup>8,14</sup> Following this, PVP monomers were cross-linked with divinyl glycol and even copolymerized with 2-hydroxyethyl methacrylate to create transparent hydrogels with refractive index, density, and viscosity close to the human

vitreous.<sup>8,14</sup> These polymers, however, fragmented during the injection process reducing the hydrogels' mechanical properties and opacification of the materials was also detected post implantation.<sup>8,14</sup>

Other synthetic polymers were also utilized to create possible substitutes, which include, polyacrylamide (PAA), poly(glyceryl methacrylate) (PGMA), poly(2-hydroxyethyl acrylate) (PHEA), poly(2-hydroxyethyl methacrylate) (PHEMA), hydroxypropyl methylcellulose (HPMC), poly(methyl 2-acrylamidoglycolate methyl ether) (PMAGME), Pluronic F127 (P-F127), poly(vinyl alcohol) (PVA), poly(vinyl alcohol methacrylate) (PVA-MA), Adcon-L hydrogel, fluorosilicone oil, and silicone gels.<sup>7,8,13,14</sup> These materials were biocompatible and exhibited the necessary functional properties prior to injection, however, each of them fell short in some manner. Although they improved on the problems posed by semi-synthetic polymers where the materials tended to biodegrade or get bio adsorbed, they still displayed opacification, fragmentation upon injection, increases in intraocular pressure and, in some cases, inflammation leading to retinal and corneal damage.<sup>7,8,13,14</sup> Out of all the possible materials previously examined, silicone oil remains the gold standard for vitreous replacement for longer recovery periods.<sup>7,8,13,14</sup>

Although silicone oils are effective retinal tamponades, they tend to emulsify in the aqueous environment of the eye.<sup>15</sup> The emulsification process decreases as the viscosity of the oil is increased, however, it is not possible to readily inject these high viscosity oils using a syringe.<sup>15</sup> We will propose below the use of shear-thinning polymers as potential retinal tamponades to mitigate these aforementioned problems. Before doing so, it is necessary to provide some background on the viscoelastic behaviour of polymers and copolymers.

### **1-3: Rheology**

Rheology is the study of deformation of matter due to the application of a force.<sup>16,17</sup> Viscosity is a value that describes a fluid's resistance to flow.<sup>1</sup> Viscosity is a function of the material itself and is affected by temperature, pressure, shear rate, and time of exposure to shear forces. In terms of polymers in solution, their viscosity increases as their molecular weight increases during a polymerization process. This property is thus indicative of the degree of polymerization for the reaction.

#### *1-3.1: Complex and Shear viscosity*

Complex viscosity is a frequency dependant function that can be correlated to shear viscosity as a function of shear rate through the Cox-Merz relationship.<sup>18</sup> To obtain this data, a strain sweep test has to be performed to determine the linear viscoelastic region. A strain sweep test exposes the material to different strain (%) levels to determine if there are any changes occurring to the viscosity due to changes in strain. The linear viscoelastic region is a range within the strain sweep test over which the viscosity does not change with increasing strain.<sup>19</sup> Maintaining a constant strain that falls within the linear viscoelastic range during the frequency sweep test allows any changes observed in viscosity to be directly related to frequency, which in turn can be related to the shear rate.<sup>19</sup> Complex viscosity is a useful measuring tool for materials that cannot undergo traditional techniques to determine the shear viscosity.

Shear viscosity, also known as the apparent viscosity, is a measurement technique utilized for non-Newtonian fluids. It is the viscosity of material under specific shear conditions (specific shear rate).<sup>18</sup> Newtonian fluids maintain a constant viscosity when exposed to changing shear rates, however, the viscosities of non-Newtonian fluids

change with shear rate.<sup>18</sup> These fluids will be discussed in greater detail in the following section.

### *1-3.2: Newtonian and Non-Newtonian fluids*

Newtonian liquids are those that exhibit a constant proportionality when shear stress is plotted against shear strain.<sup>16</sup> This proportionality between the two values is known as the shear modulus and is maintained over the entire domain of the graph.<sup>16</sup> Furthermore, the viscosities of such materials do not vary with shear rate or time of shearing.<sup>16</sup> Non-Newtonian fluids, however, do not exhibit this same proportionality and deviate from these aforementioned characteristics.<sup>15</sup> There are two major types of non-Newtonian fluids: shear-thickening and shear-thinning.<sup>16</sup> Shear thickening materials increase their viscosity with increasing shear rate.<sup>16</sup> This type of material would be an ineffective choice as a retinal tamponade as it would be unfeasible to inject them using a syringe. A shear-thinning material is more desirable as it would exhibit the high viscosities required in the rest state to allow for an effective tamponade effect. Furthermore, the lower viscosities of these materials under a stressed state will allow them to be easily injected using a syringe. We were therefore interested in modifying silicone oils to create a shear thinning material with an enhanced ability to act as an optimal vitreous substitute.

The viscosity of shear thinning molecules decreases as the shear rate is increased.<sup>16</sup> Shear thinning molecules are categorized into two classes according to their flow curves: plastic and pseudoplastic.<sup>16</sup> Both plastic and pseudoplastic materials display a limiting high shear rate viscosity (see Fig 1-2).<sup>16</sup> A plastic material is one that displays a yield stress.<sup>16</sup> The shear viscosity of such materials continues to progressively increase as the shear rate is decreased, never attaining a constant value.<sup>16</sup> A

pseudoplastic also displays a limiting low shear rate viscosity (see Fig 1-2).<sup>16</sup> The viscosity of these materials increases as the shear rate is decreased, ultimately reaching a constant value.<sup>16</sup> The low shear viscosity plateau for the pseudoplastic materials and the high shear viscosity plateaus for both materials are known as Newtonian plateaus, since the material exhibits a constant modulus of elasticity and does not exhibit any changes in viscosity under these shear states.<sup>16</sup>

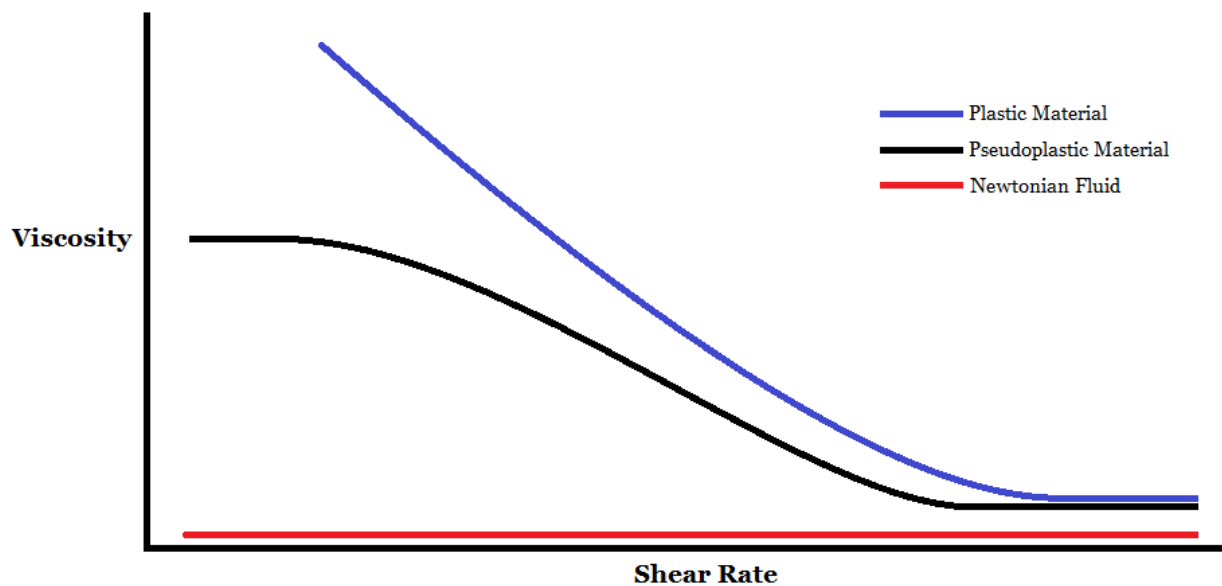


*Fig 1-2.* Shear viscosity profiles of plastic and pseudoplastic-shear thinning materials.

#### **1-4: Shear thinning materials**

Although most individuals come in touch with shear thinning materials on a daily basis, we are usually unaware of the situation. As previously mentioned, a shear thinning material is one whose viscosity decreases with increasing shear rates while displaying higher viscosities in the rest state.<sup>16</sup> Daily materials that we are commonly exposed to that are shear-thinning include latex paint, ketchup, and blood amongst many others.<sup>20-22</sup> Shear thinning materials are extremely beneficial for biomedical applications, since they allow for minimally invasive injections of various medical

treatments, including drug delivery.<sup>23</sup> The transition of high to low viscosity allows the materials to be injected with a narrow gauge syringe rather than performing larger incisions to inject more viscous materials.<sup>23</sup>

### **1-5: Measurement Techniques**

To effectively determine the rheological properties of a material, a rheometer or viscometer can be utilized. The main types of viscometers are rotational or capillary.<sup>24</sup> Viscometers are used for Newtonian fluids that do not exhibit a change in viscosity under varying flow conditions.<sup>24</sup> To analyze the rheological properties of non-Newtonian fluids, a rheometer is required.<sup>24</sup> A rheometer is able to collect data for the materials over a wide range of shear rates with narrow gaps between each collected data point.<sup>24,25</sup> This equipment is essential because it is able to detect any changes in viscosity that occur with changing shear rates. The material that is being characterized by the rheometer lies in between two basic metal parts which effectively apply the shear force on to the material: one part moves while the other remains fixed. The parts that sandwich the material to be tested can be of various geometries including concentric cylinders, cone and plate, parallel plates etc.<sup>24,25</sup> The geometry utilized is dictated by the property of the material itself or by the test being conducted.<sup>25</sup> For really low viscosity materials the concentric cylinders geometry is utilized. Materials with higher viscosities could be tested using a cone and plate geometry. As the viscosity increases even more, the parallel plate geometry is utilized for rheological testing.

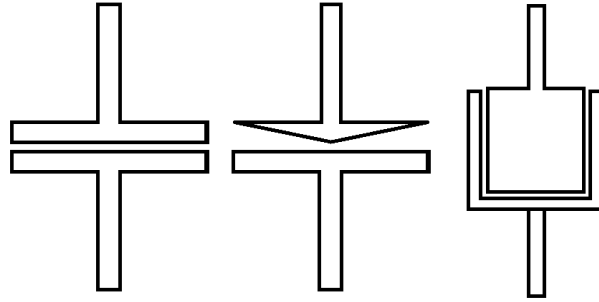


*Fig. 1-3:* Schematic representations of the different geometries (from left to right: parallel plate, cone and plate, and concentric cylinders) of the rheometers utilized for rheological testing.

### **1-6: Proposed Preparation of Shear Thinning PDMS-PEG Copolymers**

To test the proposal that it might be possible to prepare shear thinning polymers utilizing PEG and PDMS, it is first necessary to assemble such structures. The chemistry to synthesize these materials and a brief discussion of the nature of block copolymers is provided below. Prior to that, we examine the properties of silicones and PEG.

#### *1-6.1: Silicones and their Biocompatibility*

Silicone-based compounds (typically polydimethylsiloxane, PDMS), have commonly been used in a wide range of biomaterials.<sup>26-28</sup> They are widely used because they are relatively inert in biological systems: they are generally non-toxic, they display good thermal and oxidative stability, they are compatible with blood, and because of they are not adhesive to hydrated surfaces.<sup>26-28</sup> Common medical devices made from PDMS include mammary prostheses, cardiac pacemaker leads, blood pumps, artificial skin, contact lenses, medical adhesives, drug delivery systems, finger joints, catheters and many more.<sup>26-29</sup>

#### *1-6.2: Silicone oil retinal tamponade*

Silicone oils belong to the class of silicon-based polymers. Silicone oils, normally PDMS, exhibit many of the characteristics that are expected of an ideal vitreous



substitute which include being transparent, non-absorbable and non-degradable in a biological system, non-traumatic post implantation, and are injectable without degradation of the material.<sup>7,8,13,14</sup> However, more is required for the perfect vitreous substitute and silicone oils fall short of that goal.<sup>7,8,13,14</sup> Silicone oil has a refractive index of ~1.40, significantly different from the natural vitreous (~1.33).<sup>7,8,13,14</sup> This difference causes blurry vision when the silicone oil is in the eye. Furthermore, silicone oils have a lower density (0.97-0.98) than the natural vitreous, thus creating a challenge in the annealing process of the inferior portion of the retina, since the oil will rise in the aqueous environment.<sup>7,8,13,14</sup>

As previously mentioned, the greatest problem posed by silicone oils is that they are hydrophobic in nature and can be emulsified by proteins in the hydrophilic environment of the posterior chamber of the eye.<sup>15,30</sup> These emulsified globules can travel to the anterior chamber of the eye and mechanically obstruct the trabecular meshwork.<sup>15,30,31</sup> The blockage reduces the outflow capacity of the anterior chamber fluid (aqueous humour) leading to an increase in intraocular pressure thereby increasing the risk of secondary open-angle high tension glaucoma.<sup>15,30,31</sup>

Research has shown that higher viscosity silicone oils display a lower emulsification rate in the eye.<sup>15</sup> Once the silicone oil is injected, an incomplete emulsion is created with an interface between two immiscible liquids.<sup>15</sup> At the interface when additional kinetic energy (movement of the eye) is input, small globules tend to break off from larger oil droplets.<sup>15</sup> However, higher molecular weight (and, in turn, higher viscosity) silicone oils tend to resist this process via molecular entanglements.<sup>15</sup> ‘Molecular entanglements’ refers to sections of the polymer chains becoming physically coiled around neighbouring chains.<sup>15</sup> These entanglements restrict the migration of the

polymer chains from each other and thus limit the motion of one chain with respect to the other.<sup>15</sup> Lower molecular weight silicone oils display this effect to a lesser degree compared to higher molecular weight silicone oils.<sup>15</sup> This greater mobility of the lower molecular weight oils facilitates the emulsification process, posing an increased risk to the health of the treated patients.<sup>15</sup>

Based on this understanding, higher viscosity oils perform better as retinal tamponades, as they help mitigate the emulsification process. The current practical limit for injection by hand is about 5000 cSt, the viscosity of the silicone oil that is currently used as a retinal tamponade. Even the higher viscosity silicone oils with even lower tendencies to emulsify would require a mechanical pump to be injected into the eye. This process would increase the cost of the medical procedure to introduce the high viscosity oils into the eye. Shear thinning materials should be able to tackle this issue effectively, since they should be able to handle both problems amicably. Shear thinning materials exhibit high viscosity at a rest state – and hopefully resist emulsification – and when the materials undergo a shear force, their viscosity will decrease to make them more fluid and easily injectable.<sup>16</sup>

### *1-6.3: Silicone oil preparation*

A common method of creating large molecular weight PDMS compounds is via a ring opening polymerization reaction (see Fig 1-4).<sup>32,33</sup> An example of this is an acid-catalyzed reaction, where octamethylcyclotetrasiloxane (D4) is mixed with 1,1,3,3-tetramethyldisiloxane (TMDS).<sup>32,33</sup> This reactions yields a hydride-terminated PDMS compound.<sup>32,33</sup> The hydride terminal ends can then be reacted with other compounds to create the desired product (see Fig 1-4). The ratio of D4 to TMDS helps determine the molecular weight of the resulting linear PDMS chains. With a higher proportions of D4,

one is able to obtain higher molecular weight PDMS. These higher molecular weight PDMS oils tend to have much higher viscosities due to greater intermolecular interactions.<sup>34</sup> Furthermore, the viscosity tends to increase exponentially with increasing molecular weight.<sup>34</sup>

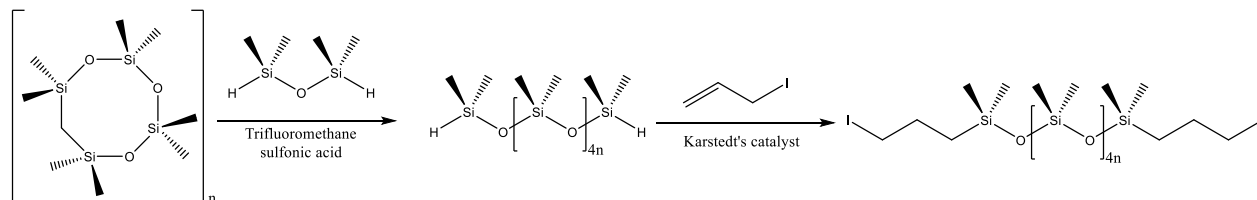


*Fig. 1-4:* Schematic representation hydride terminated PDMS synthesis followed by end group modification.

#### 1-6.4: Hydrosilylation

Hydrosilylation reactions refers to the addition across multiple bonds – double or triple bonds – in organic molecules of an SiH functional group, that maybe found in inorganic or organometallic compounds.<sup>35</sup> The reaction was first reported in 1947, and many catalysts have been created to facilitate this reaction.<sup>35</sup> The process is a generic, facile and high yielding way to generate silicon-carbon bonds. The transition metal catalysts accomplish this reaction through a heterocyclic mechanism (see Fig 1-5).<sup>35</sup> The reaction typically occurs in an anti-Markovnikov fashion, however, under certain conditions the Markovnikov product can be formed.<sup>35</sup> Typical transition metals used for this procedure include platinum (Pt), palladium (Pd), nickel (Ni), iron (Fe), rhodium (Rh), ruthenium (Ru), and copper (Cu).<sup>35</sup> Hydrosilylation reactions can also occur through free radical initiation and nucleophilic-electrophilic catalysis mechanisms.<sup>35</sup> This process can be used to graft silicone polymers to other entities, including polymers.

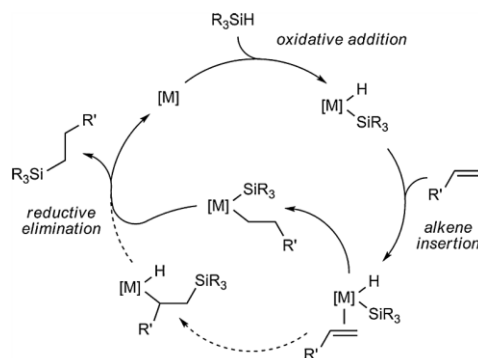


*Fig. 1-5: Generalized transition metal catalyzed hydrosilylation reaction mechanism (reproduced with permission).<sup>36</sup>*

### 1-7: Methods to Improve Hydrophilicity

Due to the hydrophobic nature of silicone oils, there is a problem with proper filling of the vitreous cavity.<sup>37</sup> The hydrophobic nature causes the material to have poor contact with the retina, thus inhibiting the ability of the oil to fully close the retinal breaks.<sup>37</sup> To aid in this procedure, it should be possible to modify the silicone oils to make them more hydrophilic and help create a better interface between the silicone polymer and its hydrophilic surroundings. This can be done by chemically tethering hydrophilic compounds to the silicone that can help mediate this issue.

The human body is an aqueous environment, as is it comprised of ~70% water.<sup>38,39</sup> Due to this reason, it is beneficial for materials introduced into the human body to be either hydrophilic or undergo some form of modification to create a hydrophilic exterior (micelle-like structure) for easier transport. In the pharmaceutical industry, poly(ethylene glycol) (PEG) is a commonly used modifier that helps to increase the hydrophilicity of compounds.<sup>40</sup> Tethering PEG compounds to silicones could, in principle, help enhance the effectiveness of silicone-based retinal tamponades, as it will increase the hydrophilicity of the otherwise hydrophobic silicone.

### *1-7.1: Poly(ethylene glycol)*

Poly(ethylene glycol) refers to synthetic polyethers made up of repeating CH<sub>2</sub>-CH<sub>2</sub>-O units with molecular weights of less than 100,000 g/mol.<sup>41</sup> At higher molecular weights the polymer is referred to as poly(ethylene oxide)(PEO).<sup>41</sup> PEG is an FDA-approved material that is non-immunogenic, non-toxic, and highly soluble in water and other many organic solvents.<sup>41-43</sup> These properties can be transferred to materials being introduced into the body by tethering PEG to them - a PEGylation process. By doing so, the materials exhibit: reduced kidney excretion and higher bioavailability, reduced degradation by proteolytic or hydrolytic enzymes, reduced immunogenic and antigenic properties, and enhanced water solubility.<sup>41-43</sup>

In an aqueous environment, PEG will form hydrogen bonds to create a hydration shell around itself. When PEG is tethered to lipophilic materials, this hydration shell will create an interface between the hydrophobic and hydrophilic system.<sup>44</sup> For the purposes of a retinal tamponade (especially silicone oil) this property could be extremely important, as it will help in the process of creating a more effective therapeutic treatment. The hydrophilic PEG will help the tamponade come closer in contact with the retinal cells, thus allowing for a better seal of the tear or detachment.

PEG can be created via anionic (see Fig. 1-6) or cationic ring-opening polymerization reactions using epoxides.<sup>45</sup> PEG can be obtained with different functional groups, including vinyl- or allyl groups, at its termini to allow for the further chemistry that is required for the tethering process. PEG terminal ends can be modified by deprotonating the hydroxyl group followed by performing an S<sub>N</sub>2 reaction (see Fig 1-6). Through this process, it is possible to create allyl-terminated PEG molecules. The

introduction of the double bond then allows the modified PEG's to be tethered to hydride terminated silicones via a hydrosilylation reaction (see Fig. 1-5).

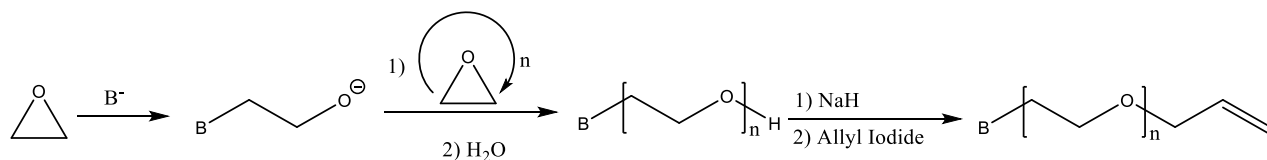


*Fig. 1-6:* Ring opening anionic polymerization scheme to create PEG followed by end group modification ( $B^-$  is  $EtMgBr$ ).

### 1-8: Block Copolymer Morphologies

Block copolymers are composed of different blocks that lead to interesting properties for the overall copolymer. The morphologies of block copolymers are directly affected by the percentage composition of the blocks themselves within the overall copolymer.<sup>46</sup> The different morphologies that a block copolymer (with two types of blocks) can exhibit are body-centered-cubic spheres, hexagonally packed cylinders, bicontinuous gyroids, and lamellae.<sup>46</sup> The self-assembly processes for these block copolymers that lead to these different morphologies are mainly due to an unfavourable mixing enthalpy.<sup>46</sup> Amphiphilic block copolymers, when exposed to solvents, display an even wider range of morphologies including, spherical micelles, rods, bicontinuous structures, lamellae, vesicles, large compound micelles, large compound vesicles, tubules, “onions”, “eggshells”, baroclinic tubules, pincushions and many more.<sup>46</sup> The morphologies of the amphiphilic block copolymer samples, for example, have been shown to be affected by the amount of water content exposed to the copolymer.<sup>47</sup>

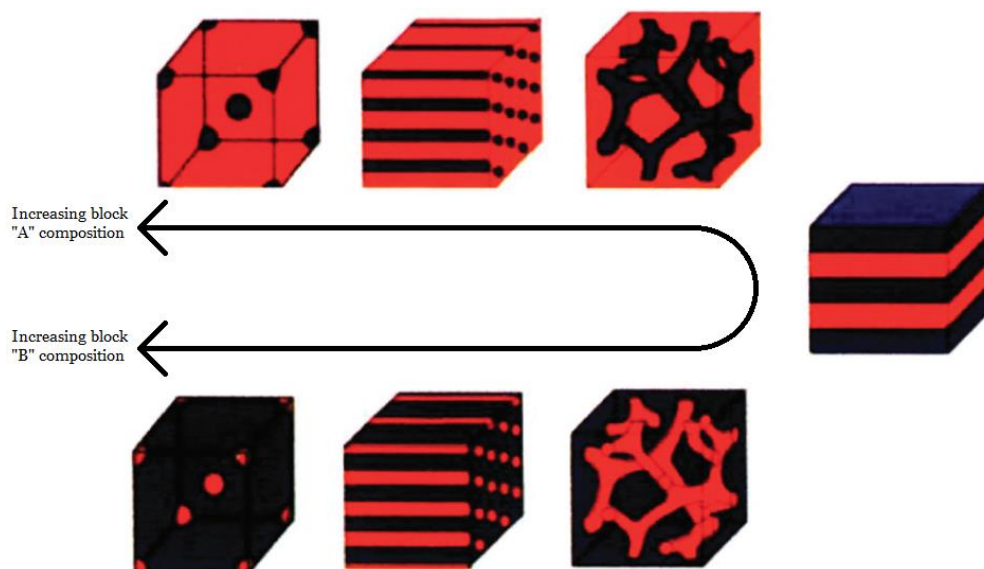


*Fig. 1-7: Block copolymer morphologies of copolymers containing two types of blocks (reproduced with permission).<sup>46</sup>*

Aside from the morphological changes that occur due to percentage composition of the copolymers, block size also affects other physical properties of the block copolymers. The degree of interaction between the blocks themselves is crucial to the viscosity of the copolymer. Higher degrees of association between the blocks (same type from different copolymer chains) help to increase the viscosity. Additionally, the viscosity of the material could be decreased by creating a situation where one block of the copolymer tends to hinder the interaction of the other block leading to a decrease in individual copolymer chain association.

## **1-9: Scope of Projects**

The goal of this project is to develop shear thinning block copolymers that can form a rigid, non-emulsifying network structure with the target of using them as retinal tamponades. Injection of a gel (or gel precursor) is not suitable, as it might be necessary in the future to remove the material from the eye. The increase in viscosity must therefore be reversible, and will arise from association of the blocks themselves. The high viscosity of these polymers in a shear free environment could also be helpful in avoiding emulsification and thus reducing the possibility of glaucoma. Furthermore, the low viscosity of the polymers in the sheared state will allow them to be injected using syringes, making the use of these materials much more practical.

For the initial part of the project (Chapter 2), block copolymers made up of PEG and PDMS with ABA and BAB configurations were synthesized and characterized. It is proposed that, with appropriate constituents, silicone and PEG blocks could associate to give shear thinning polymers with high viscosity at rest. Therefore, the molecular weights of the blocks were systematically altered to determine the effects of block size and polarity differences between the blocks on the rheological properties. To help determine the effectiveness of these copolymers, the following questions needed to be investigated:

- 1) Are the neat samples of the block copolymers shear thinning? and, Are their shear-thinning properties reversible?
- 2) Are the materials able to transmit light effectively?
- 3) Are the materials able to retain their structure and function when exposed to aqueous environments?

The first question is addressed in Chapter 2, where the neat samples are tested under different conditions. The polymers were kept anhydrous – a situation that is not relevant in the eye. The second question is addressed in both Chapter 2 and 3 for the



neat and hydrated copolymers. Lastly, question three is thoroughly investigated in Chapter 3.

## **1-11: References**

1. VanPutte C, Regan J, Russo A. Seeley's Anatomy & Physiology. New York, NY: McGraw-Hill; 2011.
2. Walton KA, Meyer CH, Harkrider CJ, Cox TA, Toth CA. Age-related changes in vitreous mobility as measured by video B scan ultrasound. *Experimental Eye Research*. 2002. 74: 173–180.
3. Bishop PN. Structural macromolecules and supramolecular organisation of the vitreous gel. *Prog Retin Eye Res*. May 2000. 19(3): 323–344.
4. Balazs EA, Denlinger JL. Aging changes in the vitreous. In aging and human visual function. Dismukes N, Sekular R, editors. pp. 45-57. New York: Alan R. Liss. 2002.
5. Larsson L, Osterlin S. Posterior Vitreous Detachment: A combined clinical and physiochemical study. *Graefe's archive for clinical and experimental ophthalmology*. 1985. 223(2): 92-95.
6. Gout I, Mellington F, Tah V, Sarhan M, Rokerya S, Goldacre M et al. *Advances in Ophthalmology*. England: InTech; 2012. Chapter 20, Retinal Detachment - An Update of the Disease and Its Epidemiology - A Discussion Based on Research and Clinical Experience at the Prince Charles Eye Unit, Windsor, England; p.341-356.
7. Soman N, Banerjee R. Artificial vitreous replacements. *Bio-Medical Materials and Engineering*. 2003. 13: 59-74.
8. Bains F. The Use of Polymers in the Treatment of Retinal Detachment: Current Trends and Future Perspectives. *Polymers*. 2010. 2: 286-322.
9. Henderer JD, Budenz DL, Flynn HW Jr, Schiffman JC, Feuer WJ, Murray TG. Elevated Intraocular Pressure and Hypotony Following Silicone Oil Retinal Tamponade for Complex Retinal Detachment Incidence and Risk Factors. *Arch Ophthalmol*. 1999. 117(2):189-195.
10. Donati S, Caprani SM, Airaghi G, et al. Vitreous Substitutes: The Present and the Future. *BioMed Research International*. 2008. 3(2): 211-218.
11. Yaszemski MJ, Trantolo DJ, Lewandrowski K, Hasirci V, Altobelli DE, Wise DL. Tissue engineering and novel delivery systems. *Rheology of biological fluids and their substitutes*. Massachusetts: Taylor and Francis; 2003.
12. Sebag J, Imaging vitreous. *Eye*. 2002. 16(4): 429-439.
13. Swindle KE, Ravi N. Recent advances in polymeric vitreous substitutes. *Exp Rev Ophthalmol*. 2007; 2(2): 255–265.

14. Baino F. Towards an Ideal biomaterials for vitreous replacement: Historical Overview and future trends. *Acta Biomaterialia*. 2011. 7(3): 921-935.
15. Crisp A, Juan E, Tiedeman J. Effect of Silicone Oil Viscosity on Emulsification. *Archives of Ophthalmology*. 1987. 105(4): 546-550.
16. Goodwin JW, Hughes RW. *Rheology for chemists: an introduction*. Cambridge: The Royal Society of Chemistry; 2008.
17. Chen DTN, Crocker JC, Wen Q, Janmey PA, Yodh AG. Rheology of Soft Materials. *Annual review of condensed matter physics*. 2010. 1: 301-322.
18. Al-Hadithi TSR, Barnes HA, Walters K. The relationship between the linear (oscillatory) and nonlinear (steady-state) flow properties of a series of polymer and colloidal systems. *Colloid and Polymer Science*. 1992. 270(1): 40-46.
19. Turi EA. *Thermal Characterization of Polymeric Materials*. 2nd Edition. Brooklyn: Academic Press; 1997.
20. Kehrwald D. Lattice Boltzmann simulation of shear-thinning fluids. *Journal of Statistical Physics*. 2005. 121(1-2): 223-237.
21. Lu CF. Latex paint rheology and performance properties. *Industrial & engineering chemistry product research and development*. 1985. 24(3): 412-417.
22. Hron J, Málek J, Turek S. A numerical investigation of flows of shear-thinning fluids with applications to blood rheology. *International journal for numerical methods in fluids*. 2000. 32: 863-79.
23. Guvendiren M, Lu HD, Burdick JA. Shear-thinning hydrogels for biomedical applications. *Soft Matter*. 2012. 8(2): 260-272.
24. Hackley VA, Ferraris CF. *Guide to rheological nomenclature: measurements in ceramic particulate systems*. National Institute of Standards and Technology, NIST Special Publication. 2001.
25. US Ink. *An Introductory Guide to Rheology*. United States: Sun Chemical Incorporated; 1995.
26. Lloyd AW, Faragher RGA, Denyer SP. Ocular biomaterials and implants. *Biomaterials*. 2001. 22(8): 769-785.
27. François B, Colas A, Thomas X. Silicones for medical use. In *XIIIth Technical Congress: Polymers for Biomedical Use*. 1996.
28. Abbasi F, Mirzadeh H, Katbab AA. Modification of polysiloxane polymers for biomedical applications: a review. *Polymer International*. 2001. 50(12): 1279-1287.

29. Lu Y, Chen SC. Micro and nano-fabrication of biodegradable polymers for drug delivery. *Advanced drug delivery reviews*. 2004. 56(11): 1621-1633.
30. Heidenkummer HP, Kampik A, Thierfelder S. Emulsification of silicone oils with specific physicochemical characteristics. *Graefes archive for clinical and experimental ophthalmology*. 1991. 229(1): 88-94.
31. Honavar SG, Goyal M, Majji AB, Sen PK, Naduvilath T, Dandona L. Glaucoma after Pars Plana Vitrectomy and Silicone Oil Injection for Complicated Retinal Detachments. *Ophthalmology*. 1999; 106(1): 169-177.
32. Brook MA. *Silicon in Organic, Organometallic, and Polymer Chemistry*. New York: John Wiley and Sons; 1999.
33. Grande JB, Fawcett AS, McLaughlin AJ, Gonzaga F, Bender TP, Brook MA. Anhydrous formation of foamed silicone elastomers using the Piers-Rubinsztajn Reaction. *Polymer*. 2012. 53(15): 3135-3142.
34. Gelest [Internet]. 2014. [cited 2014 Nov 24]. Available from: <http://www.gelest.com/goods/pdf/reactivesilicones.pdf>
35. Marciniak B. Hydrosilylation: A Comprehensive Review on Recent Advances. In: Marciniak B, editor. *Advances in silicon science*. Netherlands: Springer; 2009.
36. Troegel D, Stohrer J. Recent advances and actual challenges in late transition metal catalyzed hydrosilylation of olefins from an industrial point of view. *Coordination chemistry reviews*. 2011. 255(13):1439-1459.
37. Colthurst MJ, Williams RL, Hiscott PS, Grierson I. Biomaterials used in the posterior segment of the eye. *Biomaterials*. 2000. 21(7): 649-665.
38. Schloerb PR, Friis-Hansen BJ, Edelman IS, Solomon AK, Moore FD. The Measurement of total body water in the human subject by deuterium oxide dilution. *The Journal of clinical investigation*. 1950. 29(10): 1296-1310.
39. Garrow JS. *New Approaches to Body Composition*. *The American journal of clinical nutrition*. 1982. 35(5): 1152-1158.
40. Howard MD, Jay M, Dziubla TD, Lu X. PEGylation of Nanocarrier Drug Delivery Systems: State of the Art. *Journal of Biomedical Nanotechnology*. 2008. 4(2): 133-148.
41. Sigma Aldrich. Poly(ethylene glycol) and Poly(ethylene oxide) [Internet]. 2014 [cited 2014 Nov 25]. Available from: <http://www.sigmaaldrich.com/materials-science/material-science-products.html?TablePage=20204110>

42. Harris JM, Chess RB. Effect of pegylation on pharmaceuticals. *Nature reviews: Drug discovery*. 2003. 2(3): 214-221.
43. Veronese FM, Pasut G. PEGylation, successful approach to drug delivery. *Drug discovery today*. 2005. 10(21): 1451-1458.
44. Zolnik BS, Gonzalez-Fernandez A, Sadrieh N, Dobrovolskaia MA. Minireview: nanoparticles and the immune system. *Endocrinology*. 2010. 151(2):458-465.
45. Brocas AL, Mantzaridis C, Tunc D, Carlotti S. Polyether synthesis: From activated or metal-free anionic ring-opening polymerization of epoxides to functionalization. *Progress in polymer science*. 2013. 38(6): 845-873.
46. Mai Y, Eisenberg A. Self-assembly of block copolymers. *Chemical society reviews*. 2012. 41(18): 5969-5985.
47. Choucair A, Eisenberg A. Control of amphiphilic block copolymer morphologies using solution conditions. *The European Physical Journal*. 2003. 10(1): 37-44.

## Chapter 2: Characterization of PEG-PDMS block copolymers of ABA and BAB geometry<sup>†</sup>

### Abstract

Silicones and PEG are polymers that are commonly utilized for biomedical purposes. PEG is tethered to many compounds to help improve their hydrophilicity. Due to silicones' high permeability to oxygen, its ability to transmit light effectively, and essentially inert characteristics in a biological system, it is used as the gold standard for long term retinal tamponades. However, its hydrophobicity does not allow silicone oil to completely fill the posterior chamber. Furthermore, silicone oil tends to emulsify in the aqueous environment of the eye leading to an increased risk of secondary glaucoma. It has been shown that higher viscosity silicone oils have a lower rate of emulsification. Higher viscosity materials are, however, harder to inject and require specialized tools which increases the cost of the procedure. We attempted to tackle both of these problems by creating shear thinning block copolymers using poly(ethylene glycol) (PEG) and poly(dimethylsiloxane). It was observed that the both ABA and BAB block copolymers with larger PEG blocks displayed a greater rest viscosity and a greater decrease in viscosity when exposed to shear. Turbidity results suggested that the ABA and BAB copolymers with small PEG blocks are able to transmit light more effectively than those with larger PEG blocks.

---

<sup>†</sup> This chapter will be submitted (in a slightly different form) to Colloids and Surfaces B: Biointerfaces with the following citation, "Abidur Rahman, Tony Chen and Michael A. Brook\*, *Characterization of PEG-PDMS block copolymers of ABA and BAB geometry, Colloids Surf. B.*" I undertook all the work, with the exception of branched pendant silicone groups that were synthesized by Tony Chen and the GPC measurements which were conducted by Dr. Dan Chen.

## **2-1: Introduction**

Vision is one of the five major sensory inputs that we as human beings rely upon heavily on a daily basis. The information that is detected by the eye is transmitted from the retina, the neural portion of the eye, to the brain.<sup>1</sup> The human eye is separated into three chambers: the anterior chamber, the posterior chamber, and the vitreous chamber.<sup>1</sup> The vitreous chamber houses a gel known as the vitreous humour that helps maintain the shape of the eye, holds the retina in place, and facilitates the movement of nutrients throughout the chamber.<sup>2-3</sup> The vitreous gel is composed of ~97-99% water, and structured by the presence of small quantities of hyaluronic acid and collagen.<sup>2-4</sup> The composition of these materials tends to change over time as people age, causing the vitreous to liquefy and shrink in size.<sup>5</sup> As these changes occur the gel can pull on the retina due to vitreoretinal traction, leading to an increased risk of retinal detachment and retinal tears.<sup>6-7</sup> These problems can distort vision and even cause blindness in severe cases.<sup>6-7</sup>

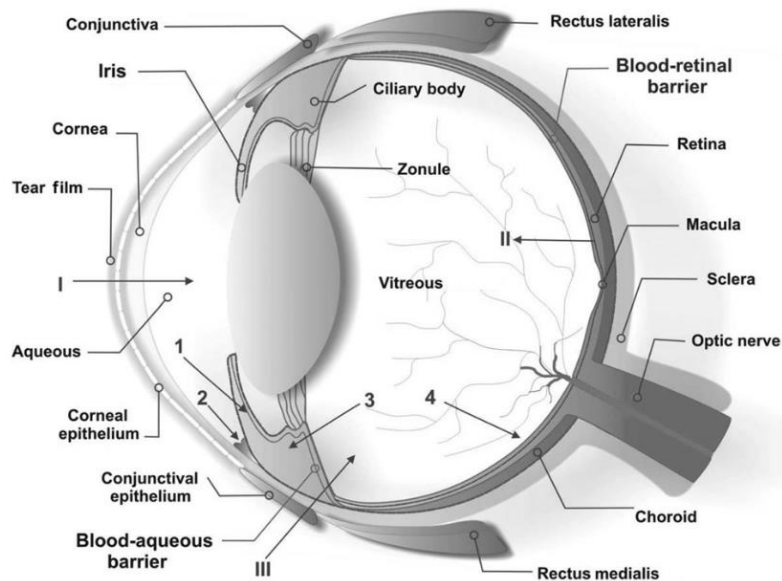


*Fig 2-1. Schematic diagram of the human eye (reproduced with permission).<sup>8</sup>*

Whenever there is an occurrence of a severe problem such as retinal detachment and retinal tears, a vitrectomy has to be performed, during which the vitreous gel is removed.<sup>2</sup> However, without the physical support of the vitreous gel it becomes difficult for the injury to heal effectively, thus a retinal tamponade is temporarily introduced to act in place of the vitreous. Many materials have been tested as potential retinal tamponades over the years including natural materials such as human donor vitreous, gases, semisynthetic materials such as modified collagen, and synthetic materials including silicone oil.<sup>2,9</sup> However, each of these materials falls short of being an optimal retinal tamponade in some way.<sup>2,9,10</sup>

The primary purpose of both long and short term vitreous replacements is to achieve a tamponade effect by holding the retina in place and sealing off any holes or tears in the tissue.<sup>2</sup> Current short term replacements that are used include gases such as perfluorocarbons and SF<sub>6</sub> (sulfur hexafluoride).<sup>2,9</sup> The gases are readily able to fill the cavity, however, they have been associated with lens opacification, increased intraocular pressure, and histopathological changes to the tissues surrounding the vitreous.<sup>2</sup>

For longer term recovery processes, silicone oils are the gold standard for retinal tamponades.<sup>2</sup> Although silicones oils are very well tolerated by the body, they fall far short of being a perfect retinal tamponade. Silicone oils are hydrophobic in nature and can emulsify in the hydrophilic environment of the posterior chamber of the eye.<sup>11,12</sup> These emulsified globules can travel to the anterior chamber and mechanically obstruct the flow of fluid through the eye, leading to an increase in intraocular pressure and increasing the risk of secondary open-angle high tension glaucoma.<sup>11-13</sup> It has also been observed that the silicone oils are unable to completely fill the posterior chamber due to



their hydrophobic nature, therefore reducing the tamponade effect, which in turn hinders the healing process.<sup>14</sup>

Previous research has shown that higher viscosity silicone oils have a lower emulsification rate than the lower viscosity silicone oils, which leads to the proposition of utilizing higher molecular weight silicone oils as retinal tamponades.<sup>12</sup> However, to use even higher viscosity materials, surgeons would require specific pumps to inject the material into the posterior chamber. This would in turn increase the cost of the procedure in addition to other disadvantages, including the difficulty of removing the tamponade. A different strategy would utilize fluids that are viscous once in the eye, but of much lower viscosity during placement in the eye, that is, shear thinning materials that can act as retinal tamponades.

Shear thinning materials are non-Newtonian fluids that exhibit high viscosity in their rest state, however, the viscosity decreases as the material is exposed to a shear force. In the case of polymers, once the threshold energy required to break the intermolecular associations between the individual chains is input into the system through the shear, the viscosity of the material starts to decrease. Once the shear force is removed, the chains once again reform the associations leading to an increase in viscosity (see *Fig 2-2*). The use of such materials would allow the tamponade to be injected using a simple syringe in the sheared state. Once inside the posterior chamber, the tamponade could return to the necessary highly viscous state.

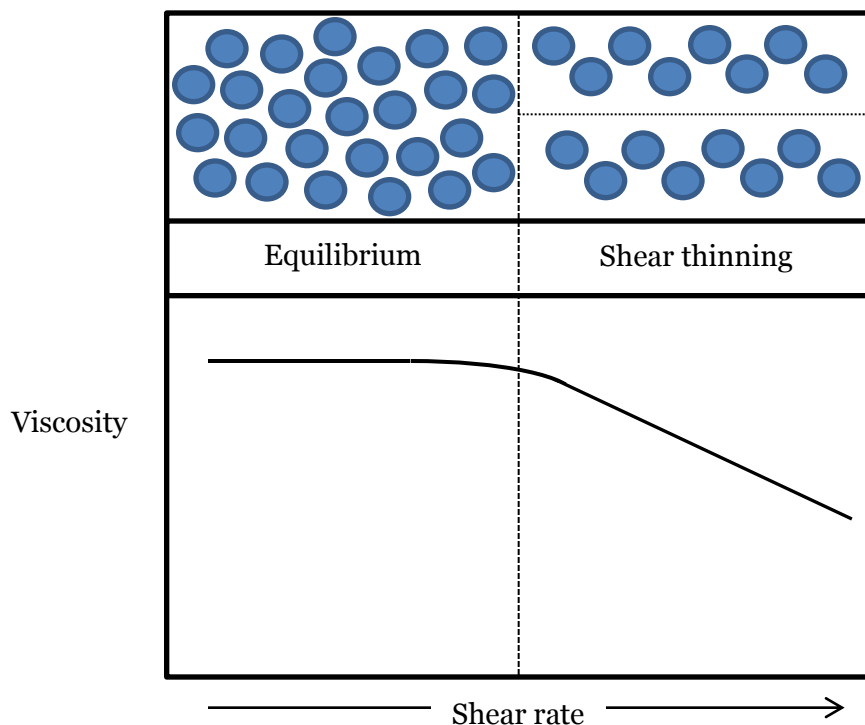


*Fig 2-2.* Schematic diagrams of rest state (left) and sheared state (right) of shear thinning copolymers.

This project aimed to develop shear thinning block copolymers that can form a rigid, non-emulsifying network structure once injected as a retinal tamponade. To do so it is necessary to design polymers of the appropriate structure(s). The individual blocks of a shear thinning block copolymer will associate with identical blocks on adjacent polymer chains. They must also be compatible (able to dissolve in the same solvent so that chemical reactions can be performed on them) with the chemically distinct blocks. Examples of previously tested shear thinning block copolymers for different biomedical purposes include polyoxyethylene-block-polyoxypropylene and acrylamide-block-benzylacrylamide.<sup>15,16</sup> In both cases, the individual blocks are relatively similar, however, the slight differences in the structural and chemical properties of the blocks are enough to allow the materials to exhibit shear-thinning properties.

Polydimethylsiloxane (PDMS) and poly(ethylene glycol) (PEG) are commonly utilized in the biomedical industry and have been thoroughly tested for their biocompatibility, making them suitable choices for materials in this application. They do not dissolve well with one another which, as noted above, is another potentially useful element for the design of shear thinning tamponades: the separation of the different blocks will provide physical crosslinking. In addition, PEG has the propensity to adsorb large quantities of water by forming hydrogen bonds, which helps to introduce hydrophilic character to the copolymer.<sup>17-19</sup> The current gold standard retinal tamponade is the 5000 cSt silicone oil. This material still has a propensity to emulsify water and form globules, which can increase the intraocular pressure. Our target was to develop shear thinning materials which display a higher viscosity than 5000 cSt (~4.9 Pa.s) at rest, but much lower viscosity under shear and not exhibit the problems with emulsification in an aqueous milieu. Therefore, we created a series of PEG-PDMS-PEG (ABA) and PDMS-PEG-P<sup>†</sup>DMS (BAB) copolymers and subjected them to rheological tests and turbidity measurements to determine their characteristics and potential utility as retinal tamponades.

## **2-2: Materials and Methods**

### **2-2.1: Materials**

The linear mono- (5-8 cSt (~850 g/mol) or 80-120 cSt (~4750 g/mol)) and di- (100 cSt (~17500 g/mol) or 500 cSt (~28000 g/mol)) hydride-terminated poly(dimethyl siloxane) (PDMS) polymers were purchased from Gelest. Gel Permeation Chromatography (GPC) was performed to determine number average molecular weight

---

<sup>†</sup>cSt is used for kinematic viscosity while Pa.s is used for dynamic viscosity. They are related to each other according to the following relationship:

$$\text{Kinematic viscosity} = \text{Dynamic viscosity} \div \text{Density of the material}$$

(Mn), weight average molecular weight (Mw), and polydispersity indexes (PDI). These were determined using Viscotek GPC system (GPCmax VE-2001) comprising of triple detectors of VE3580 RI detector, 270 dual detectors with viscometry and RALS/LALS (Right Angle Laser Light Scattering and Left Angle Laser Light Scattering); three columns of ViscoGEL I-guard-0478, ViscoGEL I-MBHMW-3078, and ViscoGEL I-MBLMW-3078 were equipped in series. Polystyrene narrow standards were used for multi detector GPC calibration. All measurements were carried out at 35°C and at a flow rate of 1.0 mL/min, using toluene as the eluent.

The branched pendant groups were created via  $B(C_6F_5)_3$ -catalyzed Piers-Rubinsztajn reaction of allyltrimethoxysilane (Aldrich) with pentamethyldisiloxane (Aldrich).<sup>20</sup> The resultant material was then reacted with a large excess of tetramethyldisiloxane (1:10) (Aldrich) via platinum catalyzed hydrosilylation reaction to form the monohydride-terminated branched pendant group (692 g/mol).

Mono-methylated poly(ethylene glycol) (PEG) polymers (350, 750, or 2000 g/mol) were purchased from Sigma-Aldrich, as was dihydroxy-terminated PEG (400 g/mol, 1000 g/mol, or 2000 g/mol). The methylated PEG polymers were used to create the ABA copolymers while the non-methylated PEG polymers were utilized to create the BAB block copolymers. The solvents for the procedures, tetrahydrofuran (THF), hexane, and acetonitrile were obtained from Caledon. Allyl bromide (Reagent grade, 97%; Aldrich), sodium hydride (60% dispersion in mineral oil; Aldrich), Karstedt's catalyst (*see Fig. 2-3*), and Wilkinson's catalyst (*see Fig. 2-3*) were obtained from Aldrich.

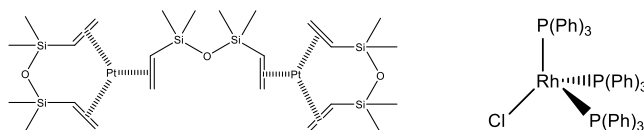


*Fig 2-3.* Schematic diagrams of Karstedt's (left) and Wilkinson's catalyst (right).<sup>21,22</sup>

## 2-2.2: Synthesis of Allylated PEG

Mono-methylated PEG was dissolved in tetrahydrofuran (~50 ml; heat was applied for the 2000 g/mol PEG dissolution for ~2 min using a heat gun while it was being stirred), to which 1.25 eq. of sodium hydride was added (Table 2-1). After the reaction mixture was stirred for 2 h under a nitrogen atmosphere, allyl bromide was added to the solution, which was then left to stir overnight (Table 2-1). A small amount of isopropanol (~1-2 ml) was added to the reaction to consume any excess hydride, following which the heterogeneous solution was filtered through Celite and cotton wool to remove the salt (sodium bromide) by-product from the reaction. To remove the hydrophobic impurities, the solution was evaporated and a liquid-liquid extraction procedure, using hexane and acetonitrile, was performed on the crude product. The purification procedure utilized acetonitrile (~15 ml) to remove the hydrophilic product from the hydrophobic impurities that remained in the hexane layer. The extraction process was performed 3 times consecutively to ensure that the all of the product was separated from the impurities. The purified monoallylated PEG was obtained after removal of solvent by evaporation from the combined acetonitrile layers. The same procedure as mentioned above was utilized to obtain the diallylated PEG, however, the latter process required 2.5 equivalents of sodium hydride and allyl bromide.

*Table 2-1: Formulation of mono- and di-allylated PEG's of various molecular weights.*

Experiment	PEG molecular weight (g/mol)	Amount of PEG (g)	Amount of NaH (g)	Amount of Allyl Bromide (ml)	Product obtained (g)	Yield (%)
Monoallylated	350	15.0738	2.1565	4.78	15.8521	94.4
	750	14.9808	1.0049	2.23	15.1031	95.7
	2000	15.0609	0.3840	0.84	14.6176	95.2
Diallylated	400	15.0230	3.7765	8.37	17.1523	95.1
	1000	14.9998	1.5213	3.35	15.3056	94.5
	2000	14.9418	0.7516	1.67	14.9685	96.3

*Chemical structures and H-NMR data for the products are available in appendix A-1.*

### 2-2.3: Linear ABA and BAB block copolymer synthesis

Platinum-catalyzed hydrosilylation was utilized to create the linear ABA and BAB block copolymers. To synthesize the ABA block copolymer, mono-allylated PEG and dihydride-terminated PDMS were dissolved in THF (~50 ml) in a 2 to 1 molar ratio (Table 2-2). Karstedt's catalyst (25  $\mu$ l of stock solution which contains 2% Pt in xylene, ~0.0011 mmol) was added to this solution, following which the reaction was left to stir under nitrogen.  $^1\text{H-NMR}$  spectra were obtained periodically to determine the degree of completion of the reaction. After completion, which typically took between 16 and 24 h, activated charcoal (~0.5 g) was added to the reaction to remove Pt from the solution. The dispersion was stirred under  $\text{N}_2$  overnight, then vacuum filtered through Celite and cotton wool. The collected filtrate was evaporated under low pressure using a rotary evaporator to obtain the desired ABA block copolymer product. The same procedure was followed to create the BAB block copolymers, however, the latter process required two equivalents of linear monohydride-terminated PDMS and one equivalent of diallylated PEG (Table 2-2).

Table 2-2: Formulations of ABA and BAB block copolymers.

Experiment	PDMS molecular weight (g/mol)	Amount of PDMS (g)	Allylated PEG molecular weight (g/mol)	Amount of PEG (g)	Product obtained (g)*
ABA	17000	12.0194	390	0.5515	11.5689
	17000	12.1502	790	1.1293	11.8638
	17000	12.1057	2040	2.9054	12.6542
	28000	12.3312	390	0.3435	11.4892
	28000	12.2188	790	0.6895	11.5728
	28000	12.1441	2040	1.7696	12.0239
BAB	850	6.1359	480	1.7325	7.1233
	850	6.1874	1080	3.9308	8.8652
	850	6.3254	2080	7.7393	12.0865
	4750	6.2256	480	0.3146	6.0878
	4750	6.1643	1080	0.7008	6.1563
	4750	6.2687	2080	1.3725	6.5243

Chemical structure and  $^1\text{H NMR}$  data for the products are available in Appendix A-2.

\*Unreacted starting materials were detected in the  $^1\text{H-NMR}$  of product which could not be separated.

#### 2-2.4: <sup>b</sup>BA<sup>b</sup>B block copolymer synthesis

The same procedure used to create the linear block copolymers was utilized to create the <sup>b</sup>BA<sup>b</sup>B block copolymers (branched pendant groups), however, the hydrosilylation reaction required a rhodium catalyst (Wilkinson's catalyst). To synthesize the <sup>b</sup>BA<sup>b</sup>B block copolymers, diallylated PEG and monohydride-terminated branched silicone based pendant group (692 g/mol) were dissolved in THF in 1 to 2 molar ratio respectively (Table 2-3). Wilkinson's catalyst (~0.02 g of a stock sample of the catalyst, 0.022 mmol) was added to this solution, following which the reaction was left to stir under nitrogen. <sup>1</sup>H-NMR spectra were used to determine the completion of the reaction. After completion, which typically took between 16 and 24 h, activated charcoal (~0.5 g) was added to the reaction to remove the rhodium catalyst from the solution. The dispersion was stirred under N<sub>2</sub> overnight, then vacuum filtered through Celite and cotton wool. The collected filtrate was evaporated under low pressure using a Rotary evaporator to obtain the desired ABA block copolymer product.

*Table 2-3: Formulations of <sup>b</sup>BA<sup>b</sup>B block copolymers.*

Experiment	Allylated PEG molecular weight (g/mol)	Amount of PEG (g)	PDMS molecular weight (g/mol)	Amount of PDMS (g)	Product obtained (g)*
BAB	480	1.9962	692	5.7557	7.2326
	1080	1.9974	692	2.5596	4.1368
	2080	3.9906	692	2.6553	5.9257

*Chemical structure and H-NMR data for the products are available in Appendix A-3.*

*\*Unreacted starting materials were detected in the H-NMR of product which could not be separated.*

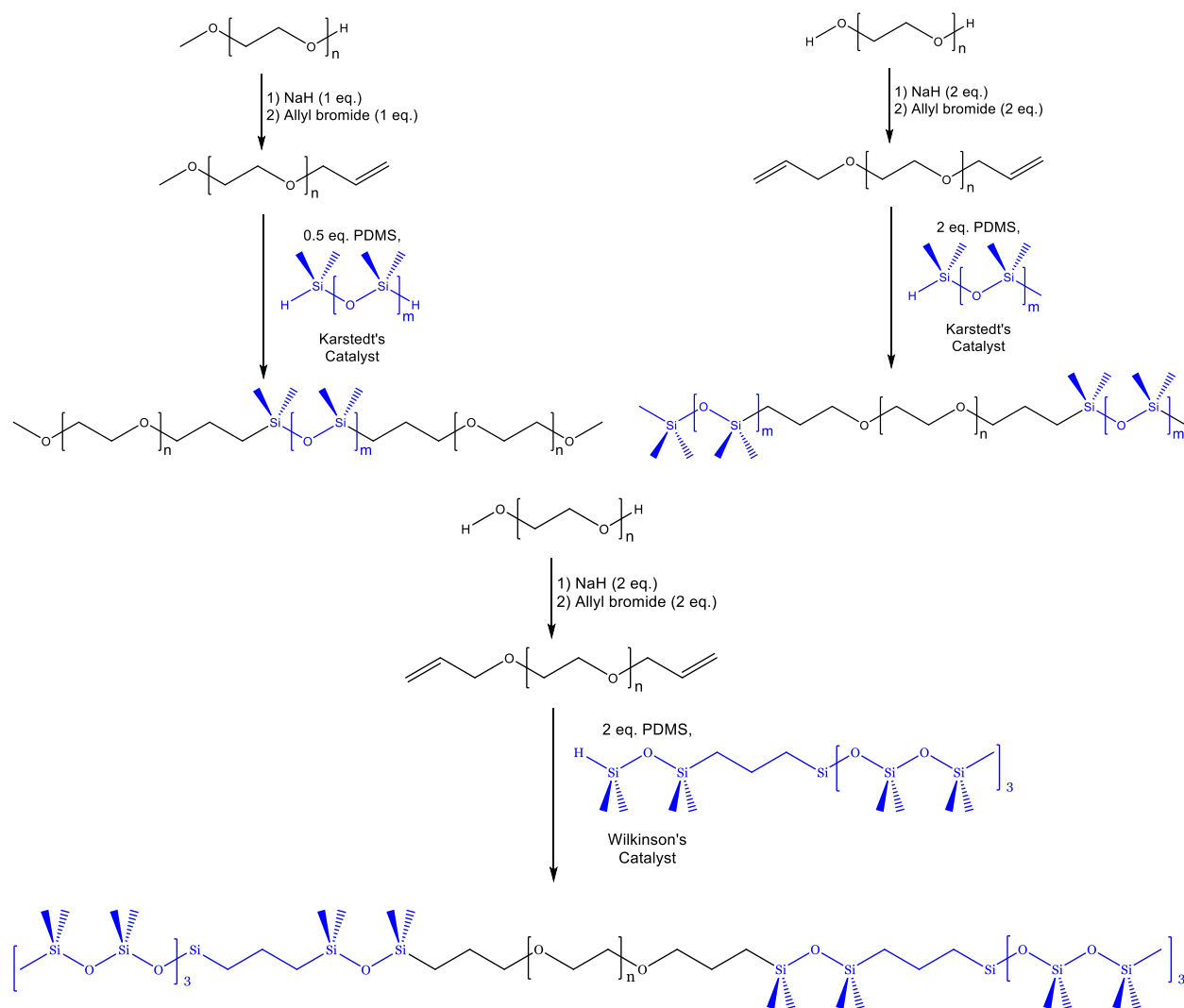


Fig 2-4. Reaction schemes for linear pendant group ABA (top left), linear pendant group BAB (top right), and <sup>b</sup>BAB (bottom) block copolymers.

Table 2-4: PEG and PDMS composition ratios for each of the block copolymer chains.

ABA Block Copolymers			BAB Block Copolymers			BAB Block Copolymers		
PEG (g/mol)	PDMS (g/mol)	PEG:PDMS ratio*	PEG (g/mol)	PDMS (g/mol)	PEG:PDMS ratio*	PEG (g/mol)	Branched Silicone (g/mol)	PEG:Branched Silicone ratio*
350	17000	~1:24.3	400	850	~1:4.4	400	692	~1:3.9
350	28000	~1:40	400	4750	~1:23.8	1000	692	~1:1.38
750	17000	~1:11.3	1000	850	~1:1.7	2000	692	~1:0.7
750	28000	~1:18.7	1000	4750	~1:9.5			
2000	17000	~1:4.3	2000	850	~1:0.85			
2000	28000	~1:7	2000	4750	~1:4.8			

\* PEG molecular weight to PDMS molecular weight per block copolymer chain.



## **2-2.5: Characterization of the samples**

### *2-2.5.1: Rheology*

Rheology experiments were performed using an Ares rheometer from Rheometric Scientific and a Stresstech HR rheometer from Rheological Instruments. Initially, the materials were characterized using complex viscosity measurements on the Ares rheometer with a parallel plate geometry (40 mm diameter parallel plates) and ~1 mm gap width between the plates. A dynamic strain sweep test ranging from 1 % - 100% was performed to determine the linear viscoelastic region. The strain values obtained from the linear viscoelastic region were utilized to perform a dynamic frequency sweep test to determine the changes in viscosity with changing frequency. The range of frequency the materials were exposed to for the test was 0.1 rad/s to 100 rad/s. The tests were performed at room temperature (~22 °C).

To determine the dynamic viscosity of the materials, steady shear sweep tests were conducted. For materials at low viscosity (<2000 Pa.s) in the rest state, a cone and plate geometry was utilized (40 mm diameter for the base of the cone) on the Stresstech HR rheometer. For materials of higher viscosity in the rest state (>2000 Pa.s), a parallel plate geometry was used on the Ares rheometer using 40 mm diameter parallel plates.

### *2-2.5.2: Turbidity measurement*

Turbidity measurements were also conducted to better understand phase behaviour in the solutions/dispersions. To conduct this experiment, samples of the linear ABA and BAB block copolymers were plated on a 48-well plate. Approximately 0.1 g of each sample, undiluted, was placed in each plate following which the materials were exposed to the visible spectrum wavelength (400 to 700 nm) using a Tecan M1000 plate reader. Light absorbance data was obtained from this experiment at 10 nm intervals.

## **2-3: Results**

### **2-3.1: Complex viscosity measurements**

ABA block copolymers were created through hydrosilylation of a monofunctional allyl-modified PEG (A block) with  $\alpha,\omega$ -dihydride-terminated PDMS (B block) via platinum catalysis. Various molecular weights were used for both PEG and silicone blocks. The object of this research was the development of shear thinning materials that, in principle, could be used as retinal tamponades. A small library of polymers was synthesized in which the molecular weight of the central block was held fixed and the flanking PEG units were varied. Initially we examined two sets of data obtained from complex viscosity measurements for PEG-PDMS-PEG copolymers: for the following data analysis the central PDMS blocks were held constant while the terminal PEG blocks were varied in size.

Maintaining the PDMS block size at 17000 g/mol, the steady state strain sweep tests were conducted on materials with 350, 750, and 2000 g/mol PEG pendant groups. At low molecular weight PEG (350 g/mol), the test did not display any valid data: the torque values were beneath the detection limits of the instrument. As the PEG molecular weight was increased to 750 and 2000 g/mol, a linear viscoelastic region was observed followed by a decrease in viscosity with increasing strain (see Fig 2-5). Any changes in viscosity observed in the frequency sweep tests while maintaining a strain value that falls within the linear viscoelastic region can be attributed to the changes in shear rate. Strain sweep tests performed on materials with a larger central PDMS block (28000 g/mol) tethered to 350, 750, and 2000 g/mol PEG provided similar results.

Since no linear viscoelastic region was observed for the materials with the terminal 350 g/mol PEG, the frequency sweep tests were performed only on the

materials that had the 750 and 2000 g/mol PEG pendant groups. Upon performing frequency sweep tests on the materials with a central PDMS block of 17000 g/mol, a logarithmic decrease in viscosity was observed with increasing the frequency (see Fig 2-5). The material with the larger PEG (2000 g/mol) pendant groups displayed a greater decrease in viscosity compared to the materials with the smaller PEG (750 g/mol) pendant groups (see Fig 2-5). The same observation was made when the PDMS blocks size was increased to 28000 g/mol (see Fig 2-5).

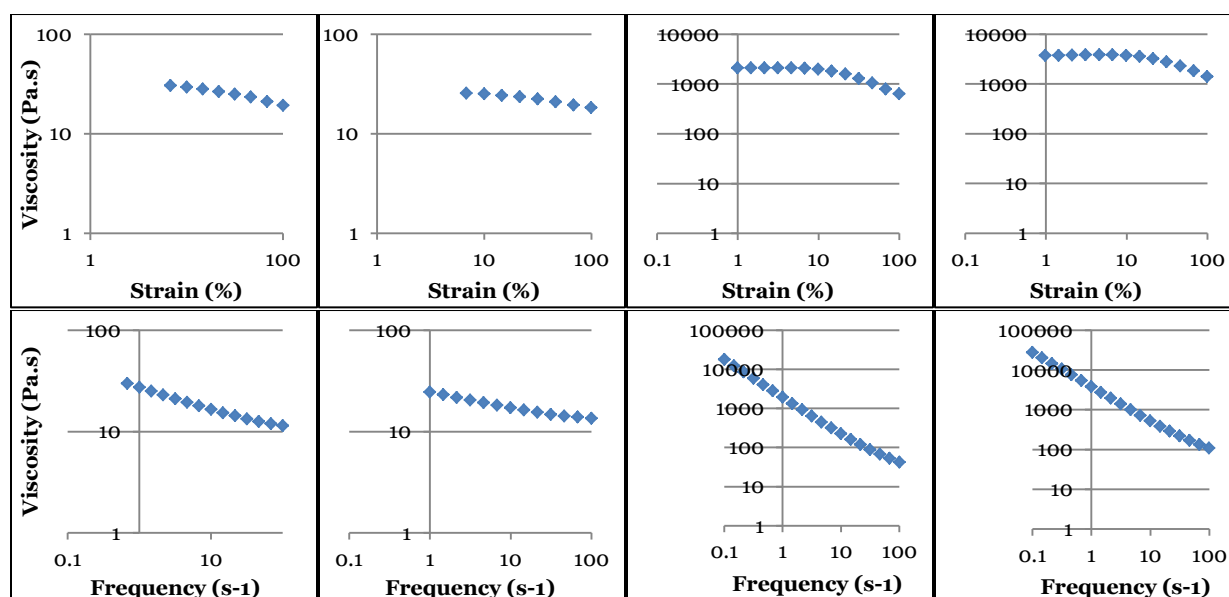


Fig 2-5. Strain sweep test data (top row) and frequency sweep test (bottom row) from left to right: ABA PEG 750 – PDMS 17000, ABA PEG 750 – PDMS 28000, ABA PEG 2000 – PDMS 17000, ABA PEG 2000 – PDMS 28000.

### 2-3.2: Shear viscosity measurements

Although the complex viscosity measurements helped to determine that the materials with higher molecular weight PEG (750 and 2000 g/mol) pendant groups are shear thinning in nature, they were unable to provide a complete picture of the changes occurring. Complex viscosity has both real and an imaginary aspects to its calculations, which prevents us from attributing specific viscosities for the material under different

shear rates (shear viscosity).<sup>23,24</sup> To determine the shear viscosities for these materials, steady shear sweep tests were conducted to give the viscosity of the materials at various shear rates. These tests were conducted on copolymers with linear central PDMS and linear terminal PEG blocks (ABA), copolymers with linear central PEG blocks and linear terminal PDMS blocks (BAB), and copolymers with linear central PEG blocks and branched terminal silicone based pendant groups (<sup>b</sup>BA<sup>b</sup>B). BAB block copolymers were created through hydrosilylation of an  $\alpha,\omega$ -difunctional allyl-modified PEG (A block) with monohydride-terminated PDMS (B block) via platinum catalysis. <sup>b</sup>BA<sup>b</sup>B block copolymers were also created through hydrosilylation of a  $\alpha,\omega$ -difunctional allyl-modified PEG (A block) with monohydride-terminated branched PDMS (B block) via rhodium catalysis (Fig 2-4). The ABA block copolymers will initially be discussed where the central PDMS block size is held constant and the terminal PEG block is varied in size.

### *2-3.2.1: Rheology of linear ABA block copolymers*

A cone and plate rheometer was utilized for the copolymers with 350 and 750 g/mol PEG pendant groups, whereas a parallel plate rheometer was utilized for the copolymer with 2000 g/mol PEG pendant groups. It was observed that each of these materials when exposed to shear displayed a gradual decrease in viscosity followed by a Newtonian plateau (not observed for the copolymers with 2000 g/mol PEG). It was also observed that by maintaining the PDMS block size at 17000 g/mol and varying the PEG size (350, 750, and 2000 g/mol, respectively) the viscosities of the materials increased with increasing PEG size (see Fig 2-6). The logarithmic drop in viscosities was greater as the PEG block size was increased in the copolymers (see Fig 2-6).

At a higher central PDMS block size (28000 g/mol), the same trend was observed: the materials with larger PEG terminal groups displayed a greater viscosity. The materials once again displayed a logarithmic decrease in viscosity with increasing shear rate, which aligns with the aforementioned conclusion that they are shear thinning materials. At the smaller PEG pendant block sizes (350 and 750 g/mol), the viscosities of the materials were greater for materials with the larger central PDMS block. However, when comparing the ABA copolymers with 2000 g/mol PEG pendant group it was observed that the reverse was true (see Fig 2-6).

### *2-3.2.2: Rheology of linear BAB block copolymers*

When the pendant silicone block was 850 g/mol, the copolymers made using 400 and 1000 g/mol PEG as the core block were tested using the cone and plate rheometer, however, the copolymer made with 2000 g/mol PEG required the usage of the parallel plate rheometer. The materials with the BAB geometry displayed a similar trend, where the viscosities were higher with increasing PEG molecular weight while the terminal silicone groups were kept constant. Each of the copolymers made from varying sizes of central PEG block tethered to 850 g/mol linear silicone pendant displayed a decrease in viscosity with increasing shear. The Newtonian plateau was only observed when the PEG size was 400 g/mol whereas it was undetected for the copolymers made with 1000 and 2000 g/mol PEG within the tested range (more energy required to sever the associations between the individual copolymers to observe the Newtonian plateau). The increase in viscosity was significantly greater as the PEG block size increased from 400 to 1000 g/mol PEG compared to the increase in viscosity from 1000 to 2000 g/mol PEG (see Fig 2-6). It was also observed that the change in viscosity with increase shear rate was greater as the PEG size increased.

When the pendant group size for the BAB block copolymers was further increased to 4750 g/mol, a similar trend was observed, where the rest viscosity was greater with increased PEG size (see Fig 2-6). However, compared to the shorter linear PDMS pendant groups (850 g/mol) the change in low shear viscosities as the PEG blocks were increased in size (400 to 1000 g/mol and 1000 to 2000 g/mol) was much smaller. Furthermore, the viscosity for the copolymer made using 400 g/mol displayed a greater viscosity when the PDMS block was larger, however, the reverse became true when the PEG size was increased to 1000 and 2000 g/mol.

### *2-3.2.3: Rheology of <sup>b</sup>BA<sup>b</sup>B block copolymers*

In the branched <sup>b</sup>BA<sup>b</sup>B copolymers, the materials made from 1000 g/mol PEG displayed lower viscosities than the analogous linear BAB copolymers made from 1000 g/mol PEG tethered to 850 g/mol linear silicone pendant groups (see Fig 2-5). However, as the PEG size was increased to 2000 g/mol the reverse became true. The <sup>b</sup>BA<sup>b</sup>B format displayed a greater viscosity compared to its linear counterparts (see Fig 2-6).

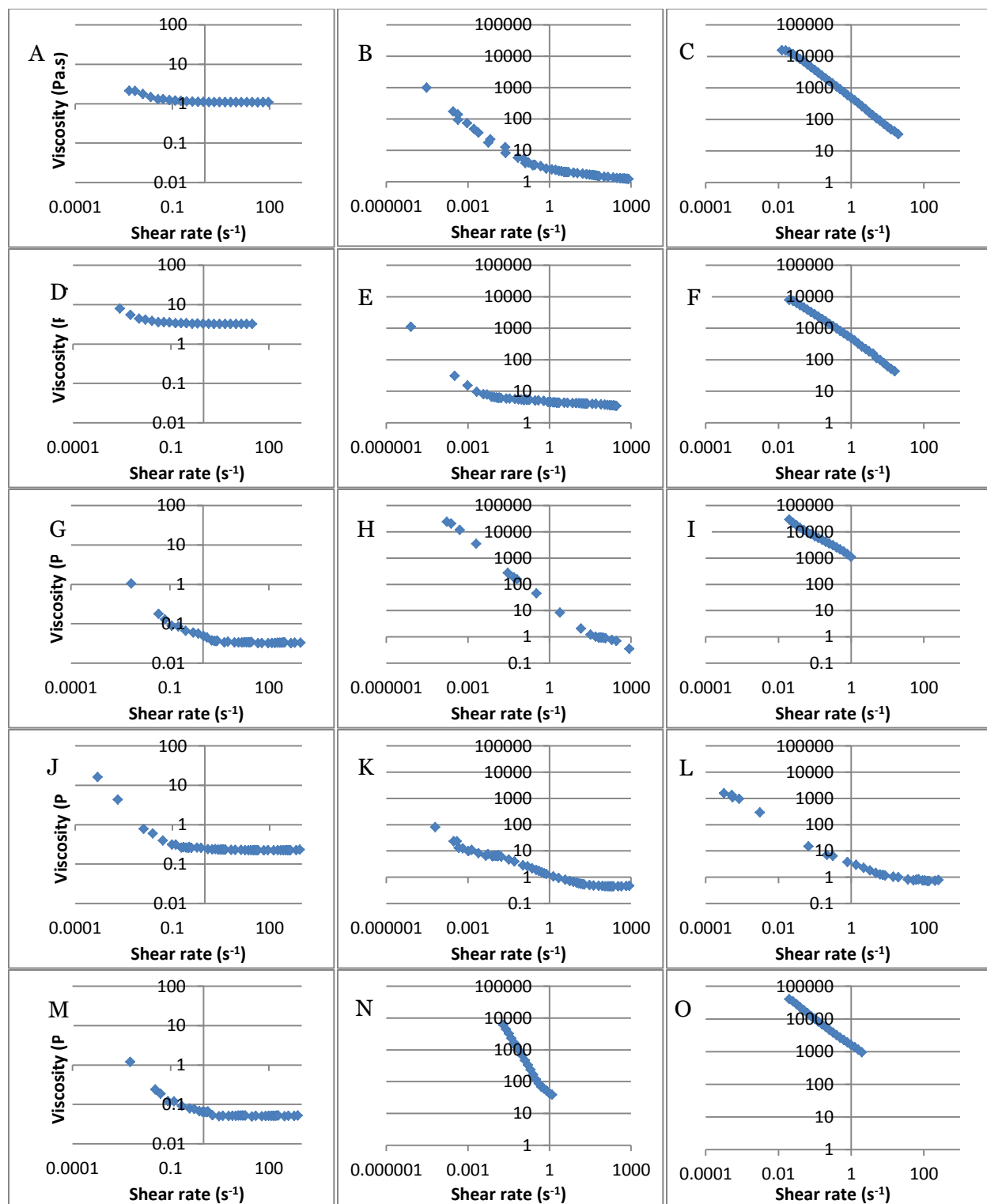


Fig 2-6. Shear sweep tests A) ABA PEG 350 – PDMS 17000 B) ABA PEG 750 – PDMS 17000 C) ABA PEG 2000 – PDMS 17000 D) ABA PEG 350 – PDMS 28000 E) ABA PEG 750 – PDMS 28000 F) ABA PEG 2000 – PDMS 28000 G) BAB PEG 400 – PDMS 850 H) BAB PEG 1000 – PDMS 850 I) BAB PEG 2000 – PDMS 850 J) BAB PEG 400 – PDMS 4750 K) BAB PEG 1000 – PDMS 4750 L) BAB PEG 2000 – PDMS 4750 M) <sup>b</sup>BA<sup>b</sup>B PEG 400 – PDMS 692 N) <sup>b</sup>BA<sup>b</sup>B PEG 1000 – PDMS 692 O) <sup>b</sup>BA<sup>b</sup>B PEG 2000 – PDMS 692.

### **2-3.3: Turbidity measurements**

The ABA, BAB, and <sup>b</sup>BA<sup>b</sup>B block copolymers exhibited higher levels of opacity as the monomer ratios of PEG:PDMS approached 1:1. These differences were quantified using light transmission through the material over the visible spectrum (400 nm to 700 nm).

#### *2-3.3.1: Linear ABA block copolymers*

The linear ABA copolymers made using 350 g/mol PEG pendant groups with varying PDMS block sizes (17000 and 28000 g/mol) were able to transmit light very successfully (>90% transmission) over the visible spectrum (see Fig 2-7). However, the copolymers that contained 750 and 2000 g/mol PEG blocks were opaque irrespective of the size of the central PDMS block.

#### *2-3.3.2: Linear BAB block copolymers*

The turbidity results for the BAB block copolymers exhibited similar results to the ABA copolymers when the PEG blocks were small. The linear BAB block copolymers made using 400 g/mol PEG were also able to transmit light very successfully (>90% transmission) over the visible spectrum. However, as the PEG size grew the trends observed in the ABA block copolymers were not followed. The copolymer containing the 4750 g/mol PDMS tethered to larger PEG blocks (1000 and 2000 g/mol) was able to transmit light over majority of the visible spectrum while the copolymers containing the 850 g/mol PDMS tethered to larger PEG blocks (1000 and 2000 g/mol) were unable to do so (see Fig 2-7). Although the materials made with larger PEG blocks (1000 and 2000 g/mol) were able to transmit light, they were far less effective at the task compared to the materials made with 400 g/mol PEG (see Fig 2-7).



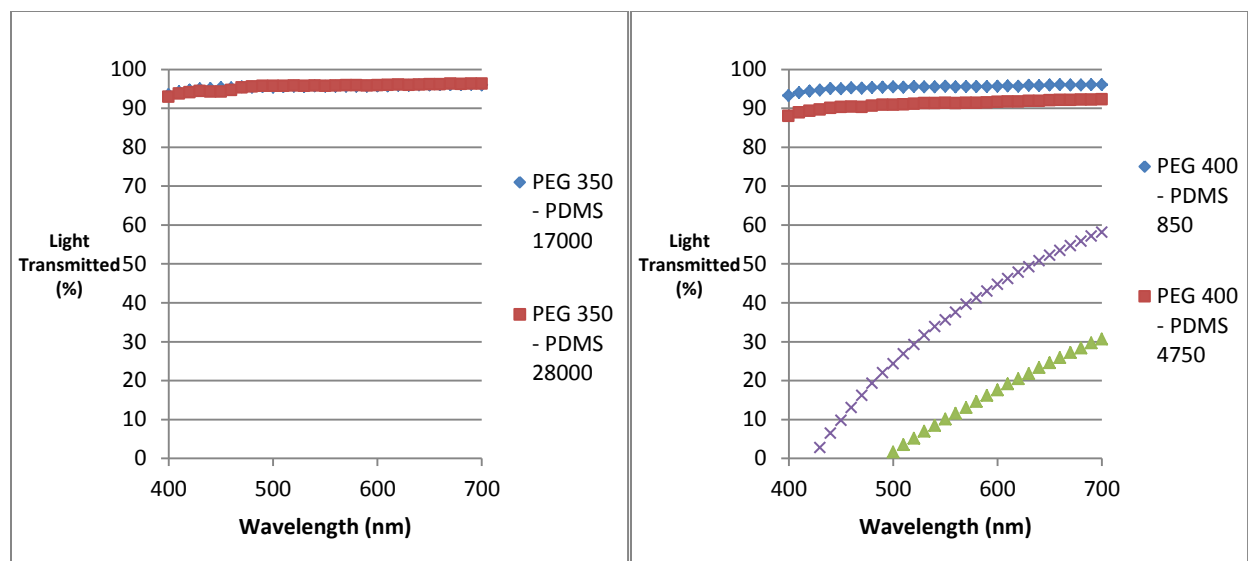


Fig 2-7. Turbidity data for linear ABA (left) and linear BAB (right) copolymers that allowed light transmission.

## **2-4: Discussion**

Silicone oil on its own does not show any changes in viscosity as function of shear unless exposed to extreme shear rates (for simple silicone oils shear rates greater than  $1000 \text{ s}^{-1}$  are required before any changes of viscosity with shear are observed).<sup>25</sup> However, the block copolymers created are significantly more sensitive to shear (viscosity changes were observed at shear rates lower than  $0.1 \text{ s}^{-1}$ ). This section examines possible origins for this difference by considering how the individual blocks, block compositions, and block geometry affect the viscosity and turbidity of the materials.

### **2-4.1: Effect of PEG molecular weight on the copolymer viscosity**

The ABA and BAB block copolymers both displayed shear thinning properties when shear sweep tests were conducted on the materials. Previous research has shown that block copolymers, with blocks that exhibit differential hydrophilicity, can possess shear thinning properties.<sup>15,16</sup> As previously mentioned, a shear thinning material has

two Newtonian plateaus where the viscosity does not change with shear. The first plateau is the region where the energy being input into the material is not sufficient to break the intermolecular bonds, and thus viscosity does not change. However, once the threshold is broken and the bonds start to be severed, the viscosity drops with increasing shear to the point where adding more energy does not change the viscosity of the materials.

It was observed in the polymers of linear ABA format that as the PEG composition per copolymer chain increased, the material displayed a greater low shear viscosity and greater decrease in viscosity with increases in the shear rate (see Fig 2-6). In our case the low shear viscosity refers to the viscosity detected at the lowest shear rate (since the first Newtonian plateau was not observed). These shear rates are comparable to the zero shear rate viscosities (rest viscosities; with the available instruments this is the lowest shear rates –  $\sim 10^{-4} \text{ s}^{-1}$  – at which data can be obtained), thus allowing us compare the viscosities between the different materials. The PEG blocks of the copolymers can form stronger intermolecular interactions based on dipole-dipole interactions, whereas the PDMS blocks associate via weaker dispersion forces. The observation that the viscosities of the materials were greater for polymers with longer PEG chains, no matter the size of the PDMS blocks, indicates that the PEG intermolecular bonds predominantly affect the viscosity. It was observed that at larger PEG blocks sizes, the viscosity decrease continues to occur at larger shear rates for materials (see Fig 2-6). This signifies that greater energy needs to be input into the system to break the larger number of PEG-PEG associations in the copolymers with larger PEG blocks.

A comparison of the role of silicone molecular weight in the ABA copolymers was established by holding the PEG size constant and varying the PDMS block size. At the smaller PEG sizes (350 and 750 g/mol), the materials with the larger PDMS block (28000 g/mol) displayed a greater viscosity. However, when the PEG size reached 2000 g/mol, the copolymer with the smaller PDMS block (17000 g/mol) displayed a greater viscosity. These differing observations can be attributed to competing effects that the silicone block has on the PEG block interactions. At the larger PEG sizes, the longer PDMS chains are most likely hindering the PEG blocks from forming optimal interactions thus leading to a decrease in viscosity (see Fig 2-8).

The polymers of linear BAB and branched <sup>b</sup>BA<sup>b</sup>B structure display similar trends: as the PEG chain increased in size the material displayed a greater maximum viscosity and greater decrease in viscosity as the shear rate increased (see Fig 2-6). This further validates that the interactions between the PEG blocks dominate structural effects on the viscosity. Furthermore, looking at the BAB copolymers, where the PEG size is kept constant while the PDMS block is varied, the copolymers with larger PEG sizes (1000 and 2000 g/mol) displayed greater viscosities when the PDMS block size was smaller (850 g/mol). In the linear ABA block copolymers, this trend reversibility (smaller PDMS block leading to greater viscosity) occurred at a smaller PEG size (at 1000 g/mol for BAB but 2000 g/mol for ABA).

The branched pendant group BAB copolymers displayed similar low shear viscosities at the smallest PEG block size (400 g/mol) compared to the linear counterparts. However, it also displayed the greatest low shear viscosity and decrease in viscosity when compared to its linear counterparts made from the largest PEG block

(2000 g/mol). In the next section we will discuss this topic in greater detail and examine the effects of geometry and copolymer composition on viscosity.

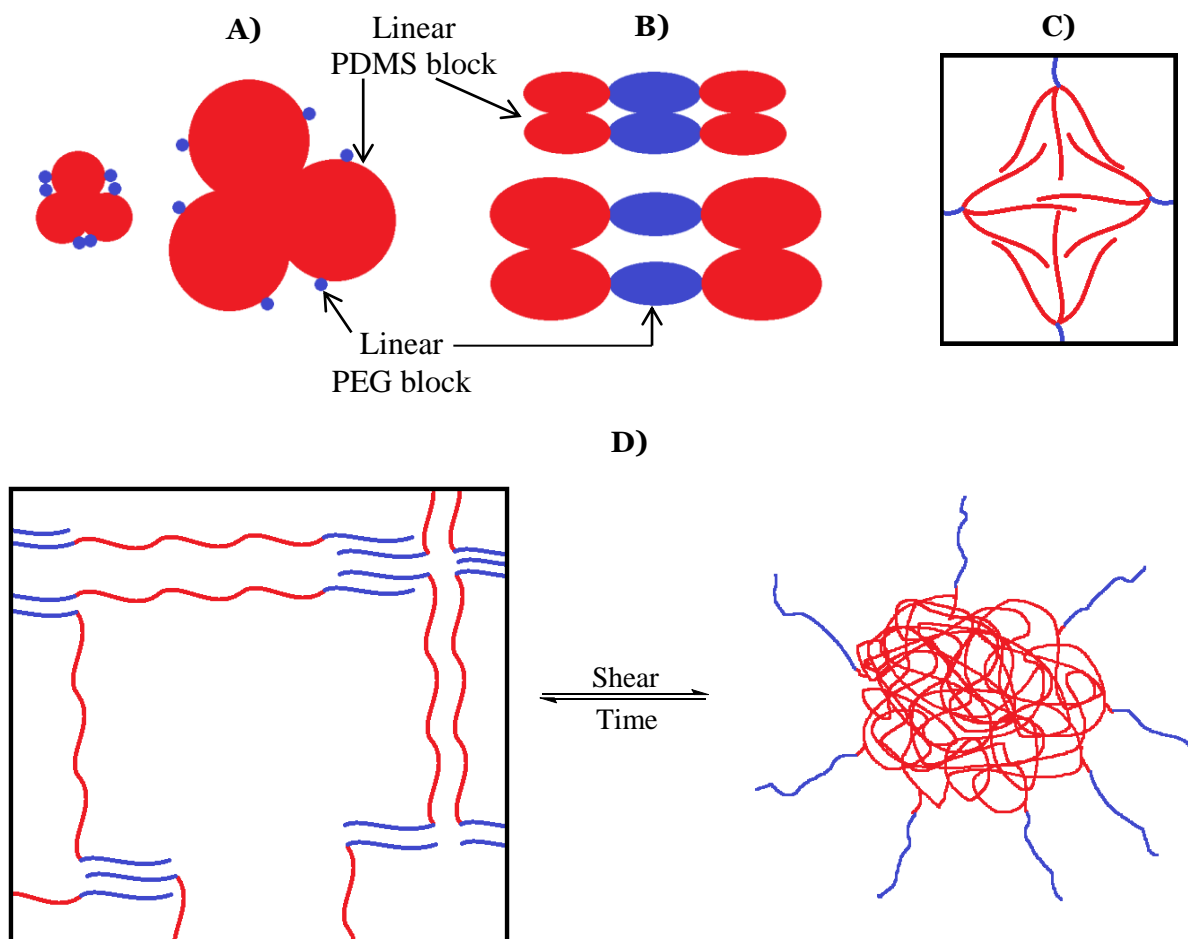


*Fig 2-8.* A) Associations of ABA copolymers as the PEG molecular weights are increased; B) Associations of BAB copolymers as the PEG molecular weights are increased; C) Association of the ordered pendant groups of the  $^b\text{BA}^b\text{B}$  copolymers; G) Change order of association between the blocks copolymers under the rest state (left) and sheared state (right).

## **2-4.2: Effect of PEG molecular weight and copolymer geometry on viscosity**

PEG content dominates the viscosity of PEG/silicone triblock copolymers because of the stronger intermolecular forces possessed by the former polymer. Looking at the compositions for the ABA vs. BAB copolymers, the ABA copolymers never displayed viscosities as high as those exhibited by the BAB copolymers (Fig 2-9). This could be because the silicone chains used in the ABA were much larger, leading to a much smaller proportion of PEG. We will examine this in greater detail in the following paragraphs.

The low shear viscosities for the linear ABA copolymers are seen to increase with increase in PEG composition (see Fig 2-9). Furthermore, the largest PEG:PDMS proportion in the ABA copolymers is ~1:4.3 whereas the PEG proportions are much greater in the BAB copolymers (see Table 2-4). When comparing ABA, BAB, and <sup>b</sup>BA<sup>b</sup>B copolymers of similar PEG ratios (ABA: PEG 2000-PDMS 17000, BAB: PEG 400-PDMS 850, and <sup>b</sup>BA<sup>b</sup>B: PEG 400 – PDMS 692; see Fig 2-6), the ABA copolymers display the greatest low shear viscosity and change in viscosity with shear rates. However, maintaining the PEG molecular weight at 2000 g/mol PEG for ABA, BAB, and <sup>b</sup>BA<sup>b</sup>B, it was observed that the <sup>b</sup>BA<sup>b</sup>B copolymer displayed the greatest viscosity. The BAB copolymers with smaller pendant PDMS chain (850 g/mol) had the second highest, then the ABA copolymers (smaller PDMS chain -17000 g/mol displayed greater viscosity), and lastly the BAB copolymer with the larger PDMS pendant chain (4750 g/mol) (see Fig 2-6). Based on these observations, it is the size of the PEG chain that has a greater effect on viscosity of the materials, not just the composition ratio. In addition, the BAB formulations tend to be more affected by the increase in PDMS size than ABA polymers. This is thought to be because the PDMS chains on the terminal ends aggregate together,

which sterically hinders the PEG blocks from associating with each other. A longer PDMS chain will create a larger aggregate, which would pose greater barrier for the PEG chain association compared to a smaller PDMS chain. With the ABA format, the PEG chains are on the terminal ends of the copolymer and thus the PEG-PEG associations are not as significantly affected by the larger PDMS block size (see Fig 2- 8).

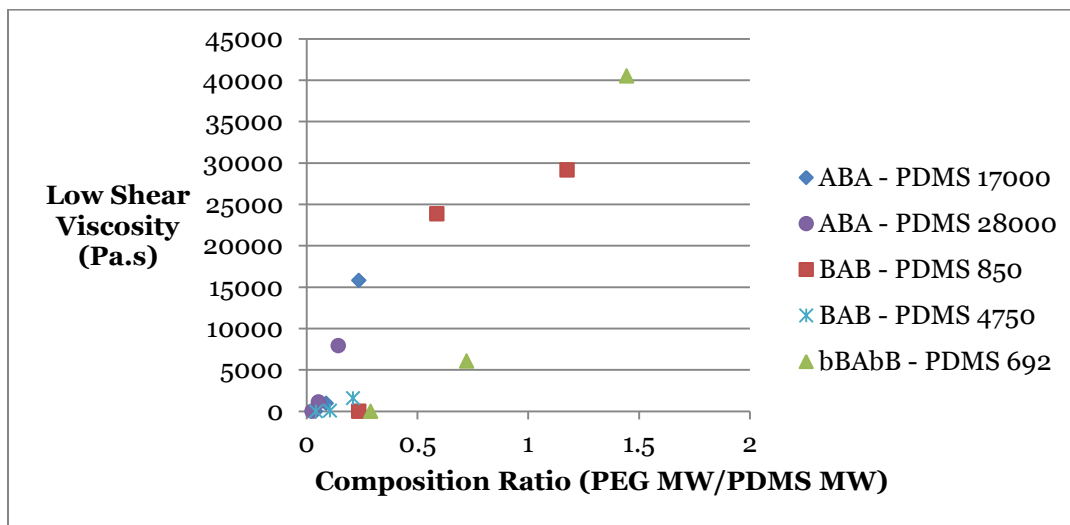


Fig 2-9. Low shear viscosities of ABA, BAB, <sup>b</sup>BA<sup>b</sup>B block copolymers.

### 2-4.3: Comparing <sup>b</sup>BA<sup>b</sup>B copolymers with linear BAB copolymers with 850 g/mol PDMS chain

A peculiar phenomenon was observed when the BAB copolymers with 850 g/mol PDMS block and <sup>b</sup>BA<sup>b</sup>B copolymers with 692 g/mol pendant group rheological data were compared. In terms of PEG and PDMS composition ratios, the copolymers are nearly the same (see Table 2-4). However, the change in viscosity as the PEG size increased was of particular interest. At 400 g/mol PEG, both of these copolymers displayed similar viscosities. Once the PEG size was increased to 1000 g/mol, the BAB copolymer displayed a greater viscosity, however, at 2000 g/mol PEG the reverse became true. It is believed that at the 1000 g/mol PEG the branched pendant groups are creating a greater steric hindrance for the PEG blocks to associate with each other. The

linear pendant groups have greater rotation freedom and are able to disperse better to allow for the PEG molecules to create better interactions with each other. However, at 2000 g/mol PEG, the terminal ends of the <sup>b</sup>BA<sup>b</sup>B copolymers have a significant amount of space between themselves thus the steric effects observed at smaller molecular weight PEG becomes negligible. At this point, it is believed that there is also an additive effect to the viscosity of the material from the branched pendant groups (see Fig 2-9). The organized branched pendant group is predicted to create interactions with the pendant groups of other chains (see Fig 2-8). In the BAB copolymers the pendant group is far less ordered, and is believed to not be able to form such ordered associations between themselves to enhance the viscosity of the material.

#### **2-4.4: Effect of PEG block size on light transmission of copolymers**

For a material to be an effective retinal tamponade it must first and foremost be able to transmit light. The turbidity measurements over the visible spectrum (400 nm to 700 nm) revealed that the opacity of the neat copolymers increased as the PEG ratio of each chain increased. The reason for the opacity is due to the difference in refractive index of the individual blocks. PEG has a refractive index of ~1.46 whereas silicones have a refractive index of ~1.40. The ABA copolymers created using the 350 g/mol PEG blocks were able to transmit light over the visible spectrum while the copolymers made from 750 g/mol and 2000 g/mol were not (see Fig 2-7). The latter copolymers had a significantly higher PEG:PDMS ratio than the copolymer with 350 g/mol PEG (see Table 2-4). This leads one to believe that when the proportion of one block of the copolymer is overwhelmingly higher in the ABA format the material is able to transmit light. The reasoning behind this statement is that, when you have a significantly higher composition ratio of one block over the other, the copolymer tends to adopt

morphologies which essentially resemble a near homogeneous mixture (for example, body centered cubic spheres). In such a case the refractive index of the block with the smaller composition plays a lesser role, since the light has a lower chance of passing through that material and being reflected or bent. However, as the block compositions become more alike, the phase separation of the individual blocks become more apparent leading the material to take on morphologies (for example, lamellar structures) that ensure that light is passing through both blocks. In this case the refractive index of both blocks of the copolymer impact light transmission through the material. If there is a significant disparity in the refractive index between the blocks in such morphologies, the light will continuously be bent and reflected, to the point where eventually no light will be transmitted. Since there is a significant difference between the PEG and silicone refractive index we see the latter case come true for the copolymers made with 750 and 2000 g/mol PEG.

In the BAB copolymers, both materials made with 400 g/mol PEG were able to transmit light at all wavelengths of the visible spectrum. The BAB copolymers made using 1000 g/mol PEG and 2000 g/mol PEG tethered to 4750 g/mol PDMS were also able to transmit light over a small range of the visible spectrum (see Fig 2-8). All of these materials had a PEG:PDMS ratio greater than  $\sim 1:4.4$ . This is likely because at greater PEG proportions (than  $\sim 1:4.4$ ), the copolymers attain a morphological structure that causes the light to bend and reflect significantly which thereby impedes light transmission through the material. Compared to the ABA format, the BAB is able to transmit light effectively at larger PEG proportions. This is probably due to the organization of the ABA copolymers vs. the BAB copolymers, where the BAB copolymers require a greater proportion of PEG to achieve morphologies where the refractive



indexes of both blocks significantly affect light transmission. Furthermore, the inability of the neat copolymers with larger PEG proportion poses a problem for them to function as retinal tamponades.

Looking at the findings from this project, it is evident that although the materials display similar rate of decrease in viscosity, it is very much possible to control the low shear viscosity for the materials by adjusting the PEG block sizes. It is also possible to affect the viscosity by altering the geometry of the pendant group and the composition of the copolymer with that specific geometry. It was also evident that the copolymers were able to transmit light when there is a significantly higher composition percentage of one block over the other. The determined parameters will help set the groundwork for future projects that are looking at creating shear thinning copolymers using PEG and PDMS. This data will to help narrow the selection of block sizes to help create materials specific for the goals at hand.

## **2-5: Conclusion**

ABA, BAB, and <sup>b</sup>BA<sup>b</sup>B PDMS:PEG copolymers were made with the idea of creating a novel retinal tamponade. The project was able to prove that the PEG and PDMS triblock copolymers do exhibit shear thinning properties. The rest viscosities of the copolymers increase with PEG block size. The association between the PEG blocks are the most important aspects to increasing the rest viscosity of the copolymers. Furthermore, the copolymers with terminal hydrophobic groups are able to exhibit far greater viscosities within the tested formulations compared to those with terminal hydrophilic groups. The terminal group geometry also plays an active role in the viscosity of the materials. Ordered branched pendant groups are able to enhance the viscosity once the central PEG chains in the <sup>b</sup>BA<sup>b</sup>B copolymers are significantly large

enough to overcome the steric effects. The associations between the branched ordered structures are far stronger than those between the long loose linear chains.

## **2-6: Acknowledgements**

I would like to thank Tony Chen for synthesizing the branched silicone based pendant group. I would also like to thank Dan Chen for helping with the GPC measurements. Lastly, I would like to thank the funding agencies: 20/20 ophthalmic network and Natural Sciences and Engineering Research Council of Canada (NSERC).

## **2-7: References**

1. VanPutte C, Regan J, Russo A. Seeley's anatomy & physiology. New York, NY: McGraw-Hill; 2011.
2. Soman N, Banerjee R. Artificial vitreous replacements. *Bio-medical materials and Engineering*. 2003. 13: 59-74.
3. Yaszemski MJ, Trantolo DJ, Lewandrowski K, Hasirci V, Altobelli DE, Wise DL. Tissue engineering and novel delivery systems. *Rheology of biological fluids and their substitutes*. Massachusetts: Taylor and Francis; 2003.
4. Donati S, Caprani SM, Airaghi G, et al. Vitreous Substitutes: The Present and the Future. *BioMed Research International*. 2008. 3(2): 211-218.
5. Walton KA, Meyer CH, Harkrider CJ, Cox TA, Toth CA. Age-related changes in vitreous mobility as measured by video B scan ultrasound. *Experimental Eye Research*. 2002. 74: 173–180.
6. Bishop PN. Structural macromolecules and supramolecular organisation of the vitreous gel. *Progress in retinal and eye research*. May 2000. 19(3): 323–344.
7. Larsson L, Osterlin S. Posterior Vitreous Detachment: A combined clinical and physiochemical study. *Graefe's archive for clinical and experimental ophthalmology*. 1985. 223(2): 92-95.
8. Willoughby CE, Ponzin D, Ferrari S, Lobo A, Landau K, Omid Y. Anatomy and physiology of the human eye: effects of mucopolysaccharidoses disease on structure and function – a review. *Clinical and Experimental Ophthalmology*. 2010. 38(s1): 2-11.
9. Bains F. The Use of Polymers in the Treatment of Retinal Detachment: Current Trends and Future Perspectives. *Polymers*. 2010. 2: 286-322.
10. Henderer JD, Budenz DL, Flynn HW Jr, Schiffman JC, Feuer WJ, Murray TG. Elevated Intraocular Pressure and Hypotony Following Silicone Oil Retinal Tamponade for Complex Retinal Detachment Incidence and Risk Factors. *Arch Ophthalmol*. 1999. 117(2):189-195.
11. Heidenkummer HP, Kampik A, Thierfelder S. Emulsification of silicone oils with specific physicochemical characteristics. *Graefe's archive for clinical and experimental ophthalmology*. 1991. 229(1): 88-94.
12. Crisp A, Juan E, Tiedeman J. Effect of Silicone Oil Viscosity on Emulsification. *Archives of ophthalmology*. 1987. 105(4): 546-550.

13. Honavar SG, Goyal M, Majji AB, Sen PK, Naduvilath T, Dandona L. Glaucoma after Pars Plana Vitrectomy and Silicone Oil Injection for Complicated Retinal Detachments. *Ophthalmology*. 1999; 106(1): 169-177.
14. Colthurst MJ, Williams RL, Hiscott PS, Grierson I. Biomaterials used in the posterior segment of the eye. *Biomaterials*. 2000. 21(7): 649-665.
15. El-Kamel AH. In vitro and in vivo evaluation of Pluronic F127-based ocular delivery system for timolol maleate. *International journal of pharmaceutics*. 2002. 241(1): 47-55.
16. Yahaya GO, Ahdab AA, Ali SA, Abu-Sharkh BF, Hamad EZ. Solution behavior of hydrophobically associating water-soluble block copolymers of acrylamide and N-benzylacrylamide. *Polymer*. 2001. 42(8): 3363-3372.
17. Sigma Aldrich. Poly(ethylene glycol) and Poly(ethylene oxide) [Internet]. 2014 [cited 2014 Nov 25]. Available from: <http://www.sigmaaldrich.com/materials-science/material-science-products.html?TablePage=20204110>
18. Harris JM, Chess RB. Effect of pegylation on pharmaceuticals. *Nature reviews: Drug discovery*. 2003. 2(3): 214-221.
19. Veronese FM, Pasut G. PEGylation, successful approach to drug delivery. *Drug discovery today*. 2005. 10(21): 1451-1458.
20. Grande JB, Fawcett AS, McLaughlin AJ, Gonzaga F, Bender TP, Brook MA. Anhydrous formation of foamed silicone elastomers using the Piers-Rubinsztajn Reaction. *Polymer*. 2012. 53(15): 3135-3142.
21. Lewis LN, Stein J, Gao Y, Colborn RE, Hutchins G. Platinum catalysts used in the silicones industry. *Platinum Metals Review*. 1997. 41(2): 66-74.
22. Burgess K, Van der Donk WA, Westcott SA, Marder TB, Baker RT, Calabrese JC. Reactions of catecholborane with Wilkinson's catalyst: implications for transition metal-catalyzed hydroborations of alkenes. *Journal of the American Chemical Society*. 1992. 114(24): 9350-9359.
23. Al-Hadithi TSR, Barnes HA, Walters K. The relationship between the linear (oscillatory) and nonlinear (steady-state) flow properties of a series of polymer and colloidal systems. 1992. 270(1): 40-46.
24. Barnes HA, Hutton JF, Walters K. An introduction to rheology. Amsterdam: Elsevier; 1989.
25. Gelest [Internet]. 2014. [cited 2014 Nov 24]. Available from: <http://www.gelest.com/goods/pdf/reactivesilicones.pdf>

## **Chapter 3: Characterization of hydrated PEG-PDMS block copolymers of ABA and BAB geometry<sup>§</sup>**

### **Abstract**

Many natural, semi-synthetic, and synthetic materials have been tested as suitable substitutes for the human vitreous. Most were found to be inadequate since they lose their structure and other desired characteristics once placed into the eye. Silicones and PEG are polymers that are commonly utilized for biomedical purposes. Silicones are currently used as the gold standard for long term retinal tamponades, however, silicone oil, due to its hydrophobic nature, tends to emulsify in the aqueous environment of the eye leading to an increased risk of secondary glaucoma. PEG has the propensity to adsorb water by forming hydrogen bonds and increasing the hydrophilicity of materials, a property that could potentially ameliorate the challenges of silicones in the eye. An array of different shear thinning triblock copolymers made of poly(ethylene glycol) (PEG) and poly(dimethylsiloxane) of both ABA and BAB geometry were exposed to various levels of hydration to determine if they are able to retain their structure and rheological properties in an aqueous environment. It was observed that both ABA and BAB block copolymers with larger PEG blocks were able to retain their structure under higher water content, unlike the analogues that possess smaller PEG blocks. The materials that retained their structure also displayed shear thinning characteristics. Turbidity results showed that the copolymers were able to transmit light effectively at elevated hydration levels that correlated with PEG composition ratio.

---

<sup>§</sup> This chapter will be submitted (in a slightly different form) to *Colloids and Surfaces B: Biointerfaces* with the following citation, “Abidur Rahman and Michael A. Brook\*, *Characterization of hydrated PEG-PDMS block copolymers of ABA and BAB geometry, Colloids Surf. B.*” I undertook all the work, with the exception of GPC measurements which were conducted by Dr. Dan Chen.

### **3-1: Introduction**

Our ability to observe the world on a daily basis depends upon the detection of light by the retina, which is located in the vitreous chamber of our eye. Whenever there is an occurrence of severe problems with retinal or vitreal pathologies, a vitrectomy has to be performed to remove the vitreous gel. Following the procedure, a replacement fluid is placed in the posterior chamber to maintain the shape of the eye and to allow the injury to heal effectively.<sup>1</sup> The primary purpose of both long and short term vitreous replacements is to achieve a tamponade effect.<sup>1</sup> Current short term replacements that are used include gases such as perfluorocarbons and SF<sub>6</sub> (sulfur hexafluoride). For longer recovery processes, silicone oils are more commonly used as the gold standard for retinal tamponades. Although silicones oils are very well tolerated by the body, they fall far short of being a perfect retinal tamponade. Previous research has shown that higher viscosity silicone oils have a lower emulsification rate that leads to the proposition of utilizing higher molecular weight silicone oils as retinal tamponades. Research suggests that a viscosity of 5000 cSt (~4.9 Pa.s) – the practical limit for hand injection and the viscosity of the gold standard silicone retinal tamponade – is not viscous enough to prevent emulsification.<sup>2</sup> However, to use higher viscosity materials, surgeons would require electronic pumps to inject the material into the posterior chamber. This would in turn increase the cost of the procedure.

We previously demonstrated that it is possible to create shear thinning materials that, in principle, can act as retinal tamponades. A series of ABA and BAB triblock copolymers using polydimethylsiloxane (PDMS) and poly(ethylene glycol)(PEG) were prepared that exhibited shear thinning properties with low shear viscosities up to 40000 Pa.s. When these materials were exposed to shear, the viscosities dropped

significantly (<1 Pa.s). Though the neat copolymers showed great promise they fell short of being the optimal retinal tamponade because the materials were opaque and were unable to transmit light effectively over the visible spectrum. Of course, the behaviour of a neat polymer in air is not representative of the same polymer in a biological milieu. Since the posterior chamber of the eye is an aqueous environment and given PEG has the propensity to absorb large quantities of water via hydrogen bonding (see Fig 3-1), we decided to examine the rheological behaviours of the hydrated version of the copolymers to establish if the materials are able to retain their shear thinning properties when exposed to water.<sup>3</sup> Therefore, the polymers were exposed to various concentrations of water, allowed to hydrate, and then their rheological properties measured. In addition, and as importantly for the application under consideration, the turbidity of the polymers was measured at various hydration levels.

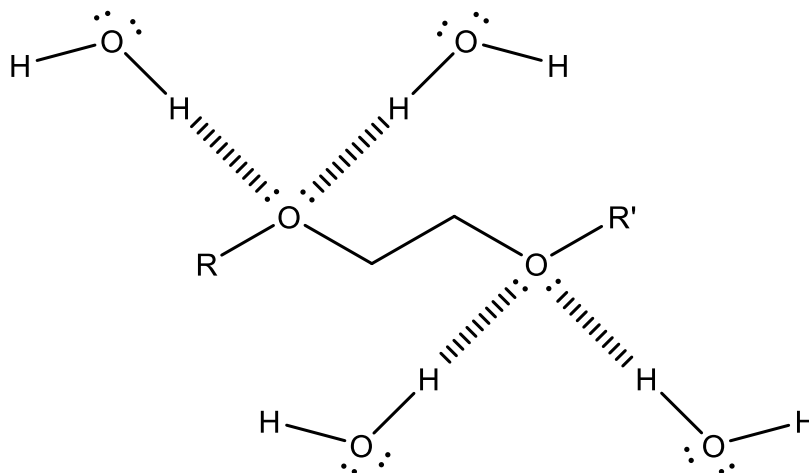


*Fig 3-1.* Schematic diagrams of PEG forming hydrogen bonds with water molecules.<sup>3</sup>

## **3-2: Experimental section**

### **3-2.1: Materials**

PEG-PDMS-PEG and PDMS-PEG-PDMS polymers were prepared as previously reported in Chapter 2. Solvents: tetrahydrofuran (THF), hexane, and acetonitrile were obtained from Caledon. Allyl bromide (Reagent grade, 97%; Aldrich), sodium hydride (60% dispersion in mineral oil; Aldrich) and Karstedt's catalyst (*Fig. 3-2*) were obtained from Aldrich and used as received. Milli-Q filtered water (18.2 M $\Omega$ .cm @ 25 °C) was utilized for the hydration of the copolymers.

Gel Permeation Chromatography was performed to determine number average molecular weight (M<sub>n</sub>), weight average molecular weight (M<sub>w</sub>), and polydispersity indexes (PDI) using a Viscotek GPC system (GPCmax VE-2001) comprised of triple detectors: VE3580 RI detector, 270 dual detectors with viscometry and RALS/LALS (Right Angle Laser Light Scattering and Left Angle Laser Light Scattering), three columns of ViscoGEL I-guard-0478, ViscoGEL I-MBHMW-3078, and ViscoGEL I-MBLMW-3078 were equipped in series. Polystyrene narrow standard was used for multi detector GPC calibration. All measurements were carried out at 35 °C and at a flow rate of 1.0 mL/min, using toluene as the eluent.

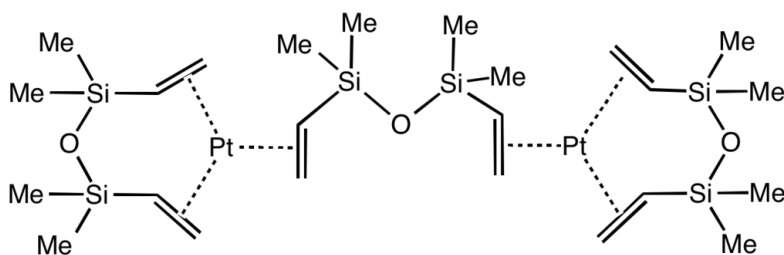


*Fig 3-2.* Schematic diagram of Karstedt's catalyst.<sup>4</sup>



### 3-2.2: Sample creation: Hydration of copolymers

Each linear copolymer (0.5 – 1 g) was weighed into a 20 ml glass vial. Four of such vials were made for each copolymer to create four different samples. Milli-Q water by volume was added using micropipettes ranging from P20 to P1000 to each vial: 1% (~0.005 – 0.001 ml), 10% (~0.05 – 0.01 ml), 100% (~0.5 – 1 ml), or the vial was filled completely (~19 – 19.5 ml) (Table 3-1). The heterogeneous solution was mixed thoroughly to allow for proper hydration using a Speedmixer DAC F150 FVZ-K for 1 min at 3000 rpm for this procedure.

*Table 3-1: Formulation of hydrated ABA and BAB copolymer samples.*

<b>Copolymer Type</b>		1% Hydration: Mass of copolymer (volume of water)	10% Hydration: Mass of copolymer (volume of water)	100% Hydration: Mass of copolymer (volume of water)	Saturated Hydration: Mass of copolymer (vial filled completely)
ABA	PEG 350- PDMS 17000	1.0256 g (0.0103 ml)	0.7380 g (0.0740 ml)	1.0333 g (1.0350 ml)	0.9984 g
	PEG 350- PDMS 28000	1.0026 g (0.0100 ml)	1.0779 g (0.1080 ml)	1.0139 g (1.0150 ml)	1.0093 g
	PEG 750- PDMS 17000	1.2464 g (0.0125 ml)	1.3527 g (0.1350 ml)	1.8282 g (1.8300 ml)	1.1326 g
	PEG 750- PDMS 28000	1.0584 g (0.0106 ml)	1.1045 g (0.1100 ml)	1.1581 g (1.1600 ml)	1.0461 g
	PEG 2000- PDMS 17000	1.0972 g (0.0109 ml)	1.0636 g (0.1060 ml)	1.1750 g (1.1750 ml)	1.1237 g
	PEG 2000- PDMS 28000	1.3232 g (0.0132 ml)	1.4049 g (0.1410 ml)	1.5630 g (1.5650 ml)	1.0118 g
BAB	PEG 400- PDMS 850	0.5165 g (0.0052 ml)	0.5106 g (0.0510 ml)	0.5399 g (0.5400 ml)	0.5005 g
	PEG 400- PDMS 4750	0.5333 g (0.0053 ml)	0.5672 g (0.0570 ml)	0.5870 g (0.5900 ml)	0.6360 g
	PEG 1000- PDMS 850	0.5338 g (0.0053 ml)	0.6353 g (0.0640 ml)	0.5220 g (0.5200 ml)	0.5230 g
	PEG 1000- PDMS 4750	0.6204 g (0.0062 ml)	0.5862 g (0.0590 ml)	0.5603 g (0.5600 ml)	0.5930 g
	PEG 2000- PDMS 850	0.5699 g (0.005 ml)	0.6277 g (0.0630 ml)	0.5089 g (0.5100 ml)	0.5837 g
	PEG 2000- PDMS 4750	0.6092 g (0.0061 ml)	0.6755 g (0.0680 ml)	0.5133 g (0.5100 ml)	0.7560 g

### **3-2.3: Characterization of the samples**

#### *3-2.3.1: Rheology*

Rheology experiments were performed using a Stresstech HR rheometer from Rheological Instruments. To determine the dynamic viscosity of the materials, steady shear sweep tests were conducted using a cone and plate geometry (40 mm diameter for the base of the cone).

#### *3-2.3.2: Turbidity measurements*

To conduct turbidity measurements, approximately 0.1 g of each hydrated copolymer was placed in a 48-well plate, following which the materials were exposed to the visible spectrum wavelength (400 nm to 700 nm) using a Tecan M1000 plate reader. Light absorbance data was obtained from this experiment with 10 nm increases in wavelength.

#### *3-2.3.3: Refractive index measurements*

Refractive index measurements were performed on the hydrated materials that exhibited high light transmission. This experiment was conducted using a Bausch and Lomb ABBE-3L Abbe refractometer. Refractive indices of the neat PEG and hydrated PEG of different molecular weights – as controls - were also obtained through this process.

## **3-3: Results**

### **3-3.1: Shear Viscosity Measurements**

ABA and BAB block copolymers were created using hydrosilylation via platinum catalysis to link monofunctional and difunctional allyl-modified PEGs (A block), respectively, with di- and monohydride-terminated PDMS (B block). Various molecular weights were used for both PEG and silicone blocks. Previous experiments proved that these linear ABA and BAB block copolymers were shear thinning when neat (Chapter 2). The objective of this research was to examine how these shear thinning properties changed with exposure to water. The polymers synthesized were small libraries in which the molecular weight of the central block was varied while the flanking pendant groups were held constant. Initially, we will examine two sets of data obtained from shear viscosity measurements of the ABA copolymers. For the following data, the terminal PEG blocks were held constant (350 and 750 g/mol) while the central PDMS block was varied in size (17000 or 28000 g/mol). The shear sweep tests for the materials were performed using a cone and plate rheometer.

After conducting the shear sweep tests, it was revealed that the hydrated copolymers displayed similar logarithmic drops in viscosities to those of the neat copolymers (see Fig 3-4). However, the infinite shear viscosities for the 1% and 10% hydrated materials (% refers to weight percent of water compared to weight of polymer) differed from the neat copolymer sample. Maintaining the PEG block size at 350 g/mol and varying the PDMS size it was observed that, at 1% hydration, the copolymers displayed a decrease in infinite shear viscosities compared to the neat sample (~1.1 Pa.s to ~0.74 Pa.s and ~3.2 Pa.s to ~1.24 Pa.s for materials with 17000 g/mol and 28000 g/mol PDMS, respectively). However, as the hydration content was increased further to

10% hydration, the infinite shear viscosities for these copolymers increased ( $\sim 2.5$  Pa.s and  $\sim 2.9$  Pa.s for materials with 17000 g/mol and 28000 g/mol PDMS, respectively) (see Fig 3-4). Shear sweep tests could not be performed on the copolymers at higher hydration levels (100% water by mass and saturated water levels), since the copolymers dispersed into small globules thereby losing their structure.

The same trend, where there is an initial decrease in infinite shear viscosity followed by an increase (with increasing hydration content), was also observed when the PEG size was increased to 750 g/mol and the PDMS size was 17000 g/mol ( $\sim 1.25$  Pa.s to  $\sim 0.95$  Pa.s to  $\sim 2.0$  Pa.s for neat, 1%, and 10% hydration) (see Fig 3-4). However, when the PDMS block size was increased to 28000 g/mol, it was observed that at 1% hydration, the infinite shear viscosity was relatively the same ( $\sim 6$  Pa.s to  $\sim 7.7$  Pa.s, for neat and 1% hydration, respectively). As the hydration level was increased to 10%, the infinite shear viscosity increased to  $\sim 22$  Pa.s (see Fig 3-4). The second set of data indicates that the threshold amount of water required to see an increase in the viscosity profile must have already been reached at 1% hydration. Similar to the copolymers with smaller PEG blocks (350 g/mol), as the hydration levels were increased further (100% water and saturated water levels) both copolymers also lost their structure.

In the BAB geometry, the shear sweep test data will be presented by examining polymers with a fixed central PEG block (400 or 1000 g/mol) with varying terminal PDMS blocks (850 or 4750 g/mol). Similar to the ABA copolymers, the BAB hydrated copolymers also retained their shear thinning properties for 1% and 10% hydrated materials (see Fig 3-4). At higher hydration levels, the materials dispersed into small globules and, thus, no shear sweep tests were performed for those samples. Maintaining the PEG block size at 400 g/mol and varying the PDMS block size, it was once again

observed that there was a drop in infinite shear viscosity at 1% hydration ( $\sim 0.04$  Pa.s to  $\sim 0.006$  Pa.s and  $\sim 0.23$  Pa.s to  $\sim 0.06$  Pa.s for materials with 850 g/mol and 4750 g/mol PDMS respectively). The viscosities once again increased at 10% hydration ( $\sim 0.05$  Pa.s and  $\sim 0.14$  Pa.s for copolymers with 850 and 4750 g/mol PDMS respectively). However, unlike the ABA copolymers, the increase at 10% hydration was lower in magnitude for the BAB copolymers with comparable sized PEG blocks (350 g/mol) (see Fig 3-4).

Similar observations were made for the BAB copolymers with 1000 g/mol PEG blocks. The infinite shear viscosity dropped from  $\sim 0.7$  Pa.s to  $\sim 0.4$  Pa.s for the copolymer with 850 g/mol PDMS and  $\sim 0.5$  Pa.s to  $\sim 0.2$  Pa.s for the copolymer with 4750 g/mol PDMS. However, unlike the previously discussed samples, the infinite shear viscosities at 10% hydration displayed little change with increased hydration ( $\sim 0.45$  Pa.s and  $\sim 0.2$  for copolymers tethered to 850 and 4750 g/mol PDMS, respectively). It is likely that greater water content is required to observe an increase in the infinite shear viscosities for the BAB copolymers with 1000 g/mol PEG block. Since the BAB copolymers have higher PEG composition ratios (see Chapter 2, Table 2-4) for copolymers with similar sized PEG blocks, greater hydration levels were required to observe the similar trend (decrease followed by an increase in infinite shear viscosity) in the viscosity profiles.

The results for the hydrated copolymers indicate that the increase in viscosity from 1% hydration to 10% hydration is higher for the copolymers with a smaller PEG composition ratio in both ABA and BAB geometry. This observation further validates that the PEG compositions of the copolymers are crucial to the viscosity changes observed. In addition, although the hydrated samples for the copolymers made with

2000 g/mol PEG in both ABA and BAB geometry were created, shear sweep tests could not be performed on these materials due to equipment restrictions.

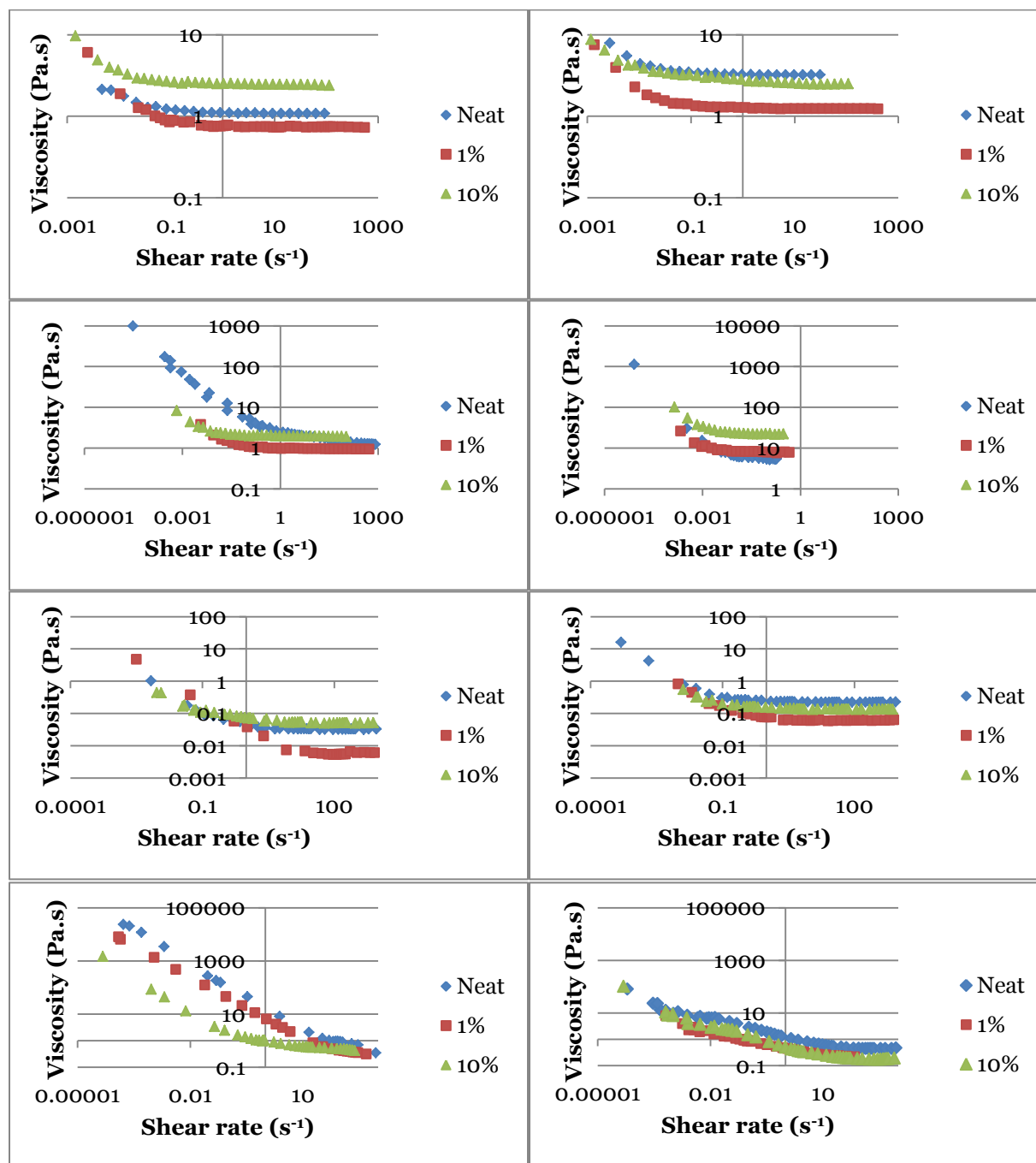


Fig 3-3. Shear sweep tests, row 1: ABA PEG 350–PDMS 17000 (left), ABA PEG 350–PDMS 28000 (right); row 2: ABA PEG 750–PDMS 17000 (left), ABA PEG 750–PDMS 28000 (right); row 3: BAB PEG 400–PDMS 850 (left), BAB PEG 400–PDMS 4750 (right); row 4: BAB PEG 1000–PDMS 850 (left), BAB PEG 1000–PDMS 4750 (right).

### **3-3.2: Turbidity Measurements**

In our previous experiments, the neat ABA and BAB copolymers increased their opacity as the PEG content per copolymer chain became similar to the PDMS content. This is due to the differences in refractive index between silicones (~1.404) and PEG (~1.46). Thus, turbidity measurements were conducted on the hydrated materials using a Tecan M1000 plate reader that calculated how much light is transmitted through the material over the visible spectrum (400 nm to 700 nm). It was observed that the materials exhibited different levels of opacity based on the size of the PEG blocks and the level of hydration. The turbidity tests were only performed on the samples that retained their structure when partly hydrated. It was observed that all the materials were able to transmit light when exposed to specific amounts of water.

#### *3-3.2.1: ABA Block Copolymers*

In the ABA copolymers, it was observed that as the PEG ratio per copolymer chain increased, higher hydration levels were required for the copolymers to transmit light effectively over the visible spectrum. Maintaining the central PDMS block size at 17000 g/mol, it was observed that the copolymer with 350 g/mol PEG was proficient at transmitting light at 1% and 10% hydration. As the PEG size increased to 750 g/mol, the proficiency decreases significantly at 1% hydration (material is still proficient at light transmission at 10% hydration) indicating that the hydration level for optimal light transmission has increased. At 2000 g/mol, the material is unable to transmit light at all at 1% hydration (only transmits light at 10% hydration) which aligns with the previous conclusion that higher PEG content per copolymer chain requires greater hydration for effective light transmission. For all these aforementioned copolymers, it was also observed that after the optimal light transmission hydration level was achieved, the

materials once again displayed high levels of opacity with increased hydration. This observation suggests that there is a specific weight percent of water that is required for optimal light transmission for each copolymer. The weight percent of water that is required for this feat is related to the PEG ratio in each copolymer chain. When the PDMS block size was increased to 28000 g/mol, the same trend was observed: as the PEG content per copolymer chain increased, greater hydration (by weight percent) was required for light transmission.

### *3-3.2.2: BAB copolymers*

Turbidity measurements were also performed on the hydrated BAB copolymers and the same trend was revealed where the copolymer's effectiveness in light transmission was directly related to its PEG composition ratio and hydration level. The BAB copolymers required greater hydration levels for optimal light transmission as the PEG composition ratio per copolymer chain were greater than the ABA copolymers with similar PEG block sizes. Maintaining the pendant PDMS block size at 850 g/mol, it was observed that as the PEG block size was increased, the level of hydration required for optimal light transmittance increased simultaneously (1% and 10% for 400 g/mol, 10% for 1000 g/mol and 100% for 2000 g/mol). As the PDMS block size was increased to 4750 g/mol, the same trend was observed. Maintaining the PEG block size constant, it was observed that the copolymer with the larger PDMS block size achieved optimal light transmittance at a lower hydration level (compare BAB PEG 2000–PDMS 4750 and BAB PEG 2000–PDMS 850, Fig 3-3). This aligns with the aforementioned conclusion that copolymers with larger PEG compositions require greater hydration to exude optimal light transmission characteristics.



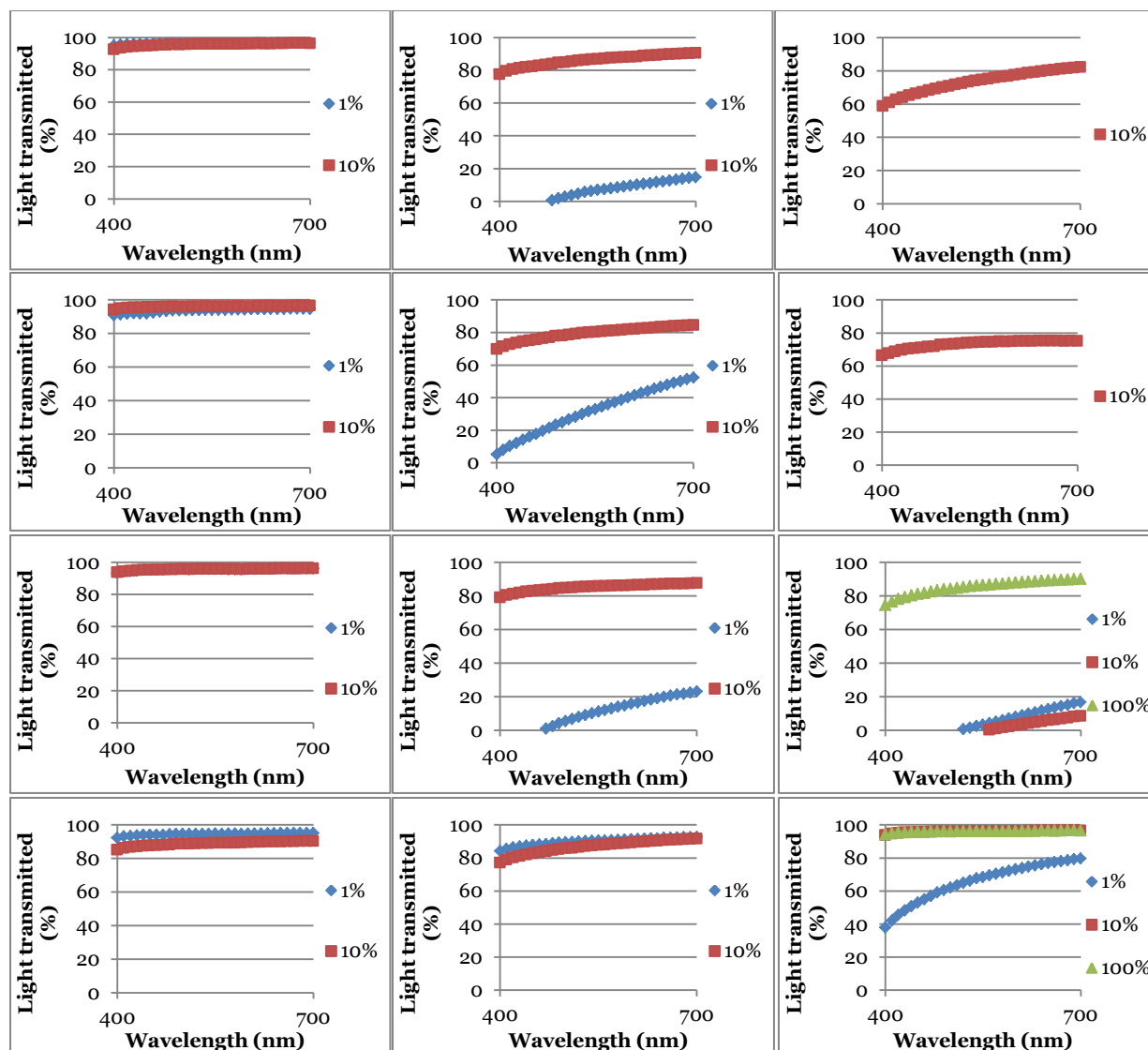


*Fig 3-4.* Turbidity data row 1: ABA PEG 350–PDMS 17000 (left), ABA PEG 750–PDMS 17000 (middle), ABA PEG 2000–PDMS 17000 (right); row 2: ABA PEG 350–PDMS 28000 (left), ABA PEG 750–PDMS 28000 (middle), ABA PEG 2000–PDMS 28000 (right); row 3: BAB 400–PDMS 850 (left), BAB PEG 1000–PDMS 850 (middle), BAB PEG 2000–PDMS 850 (right); BAB PEG 400–PDMS 4750 (left), BAB PEG 1000–PDMS 4750 (middle), BAB PEG 2000–PDMS 4750 (right).

### 3-3.3: Refractive Index for the Hydrated Polymers

In conjunction with the turbidity testing, the refractive indices of some of the materials that exhibited high light transmission were also obtained. The turbidity tests revealed that at different aqueous environments the materials appeared transparent whilst in others they seemed opaque. The refractive index of the transparent and near

transparent materials was measured using an Abbe refractometer, which revealed that the refractive index for these materials were  $\sim 1.40$  (see Table 3-2). This refractive index is very similar to that of silicone oil (1.404). PEG has a refractive index of  $\sim 1.46$ , while water has a refractive index of  $\sim 1.33$ .<sup>5</sup> In a separate experiment, pure PEG chains were exposed to increasing water content, which revealed that the refractive index slowly decreases with increasing water content (see Figure 3-5). Research conducted by other groups has also proven this phenomenon where the refractive index eventually becomes similar to that of water once the water quantity is significantly higher than the amount of PEG (lower than 1:19 PEG:H<sub>2</sub>O ratio).<sup>6</sup> These results lead one to understand that the water solvated PEG blocks in the triblock polymers could have attained a refractive index similar to that of silicone oil. This would only occur when there is an equal amount PEG and water ( $\sim 1:1$  ratio of PEG:H<sub>2</sub>O), thus causing the block copolymer to appear transparent, that is, a case of refractive index matching.<sup>7</sup>

*Table 3-2: Refractive index measurements of hydrated copolymers that exhibited high light transmission.*

<b>ABA</b>		<b>BAB</b>	
<b>Copolymer (hydration level)</b>	<b>Refractive Index</b>	<b>Copolymer (hydration level)</b>	<b>Refractive Index</b>
350 g/mol PEG – 17000 g/mol PDMS (1%)	1.4055	400 g/mol PEG – 850 g/mol PDMS (1%)	1.4140
350 g/mol PEG – 28000 g/mol PDMS (1%)	1.4065	400 g/mol PEG – 4750 g/mol PDMS (1%)	1.4055
750 g/mol PEG – 17000 g/mol PDMS (10%)	1.4051	1000 g/mol PEG – 850 g/mol PDMS (10%)	1.4180
750 g/mol PEG – 28000 g/mol PDMS (10%)	1.4050	1000 g/mol PEG – 4750 g/mol PDMS (10%)	1.4030
2000 g/mol PEG – 17000 g/mol PDMS (10%)	1.4081	2000 g/mol PEG – 850 g/mol PDMS (100%)	1.3945
2000 g/mol PEG – 28000 g/mol PDMS (10%)	1.4080	2000 g/mol PEG – 4750 g/mol PDMS (10%)	1.4080

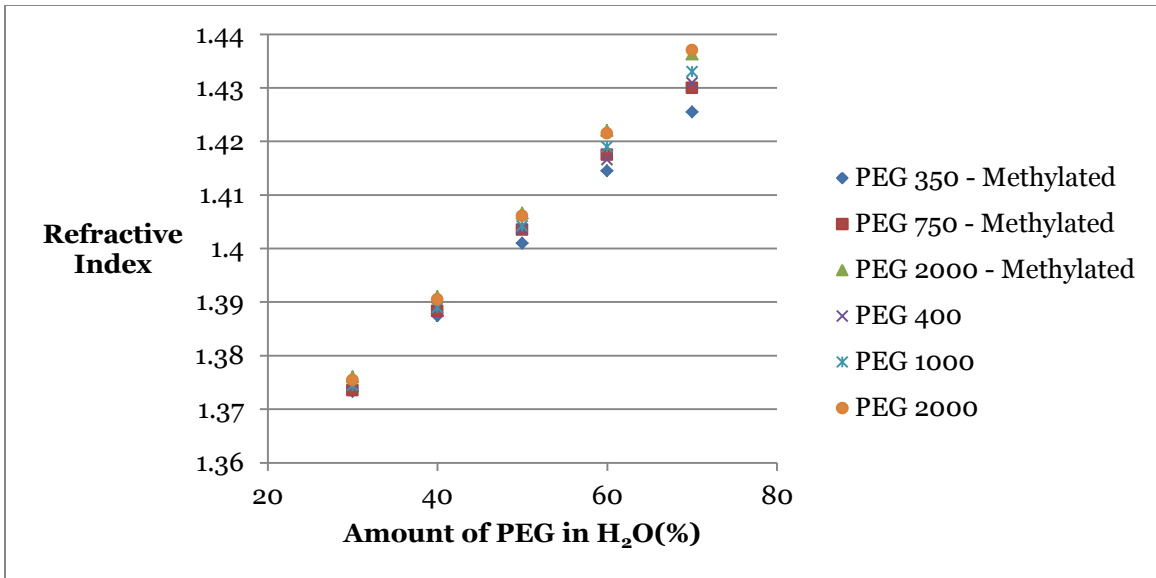


Fig 3-5. Refractive indices of PEG at various hydration levels.

### **3-4: Discussion**

Through our previous research, it was proven that multiple ABA and BAB block copolymers created using PDMS and PEG molecules were shear thinning. Previous research conducted by other groups have shown that the materials created to act as retinal tamponades lost their structure or functionality once injected into the aqueous environment of the vitreous chamber.<sup>8,9</sup> To determine if the previously established shear thinning ABA and BAB materials could retain their functionality and structure (physical association) upon hydration, the copolymers were exposed to different levels of water (from 0-100wt% and also placed in an excess of water). This section examines the effects of hydration on the copolymers in greater detail in regards to block compositions (wt% of PEG and PDMS per copolymer chain) and block geometry (ABA vs. BAB). The effects of hydration on the shear viscosity of the copolymers will initially be discussed.

#### **3-4.1: Shear Viscosity of the Linear Hydrated Copolymers**

The copolymers were created with the intention to use them as retinal tamponades. Since the vitreous chamber of the eye is an aqueous environment, shear

sweep tests were performed on the hydrated copolymers to ensure that they retained their shear thinning properties. It was observed that the ABA and BAB linear copolymers that maintained their structure (did not form a dispersion) once hydrated, exuded shear thinning properties. These results helped to ensure that these copolymers are likely to retain their shear thinning properties once they are injected in the eye. When the results of the materials were more closely inspected, a particular phenomenon was observed. The infinite shear viscosities of the hydrated materials changed with increasing hydration content. In Chapter 2, it was established that the PEG-PEG association plays the most important role in the copolymer viscosity. Any disruption in these PEG-PEG associations will impact the copolymer's viscosity. It is also understood that water molecules can partake in hydrogen bonding with the PEG block. By forming these associations, the initial PEG-PEG dipole bonds will be severed thereby impacting the viscosity of the materials.

In the shear sweep tests, it was observed that with the addition of small quantities of water (1 wt%) to the ABA and BAB copolymers, there is a drop in the infinite shear viscosities. It is believed that as small quantities of water are added, the water molecules start to form hydrogen bonds with PEG blocks of the copolymer chains. As the hydrogen bonds are formed, the PEG-PEG associations decrease which allows the PEG blocks to slip by one another. Consequently, the viscosity of the materials decreases due to the allowance of increased mobility as more PEG-PEG associations (dipole-dipole bonds between PEG blocks) are severed (see Fig 3-6). However, following this decrease, as more water (10 wt%) was added the infinite shear viscosities of the materials increased. Hydrogen bonds are stronger intermolecular forces than dipole-dipole bonds. As the dipole-dipole bonds between the PEG blocks are being severed, they are slowly

replaced with hydrogen bonds, which hold the PEG blocks close together. At a certain point of the replacement process, the association that was lost due to the severed dipole-dipole bonds is overcome by the bridging hydrogen bonds. At this point, the viscosity will start to increase (see Fig 3-3) since the water molecules will essentially form droplets which are being anchored by the PEG blocks (swollen PEG blocks). Since hydrogen bonds are stronger than dipole-dipole bonds, after a certain level of hydration, the viscosity of the hydrated copolymers will be higher than their neat counterparts (see Fig 3-3, ABA PEG 350–PDMS 17000 and BAB PEG 400–PDMS 850). As the hydration content is increased to higher levels, the materials eventually lose their structure completely due to the significant distance between the blocks, leading to a complete separation of the individual copolymer chains (see Fig 3-6).

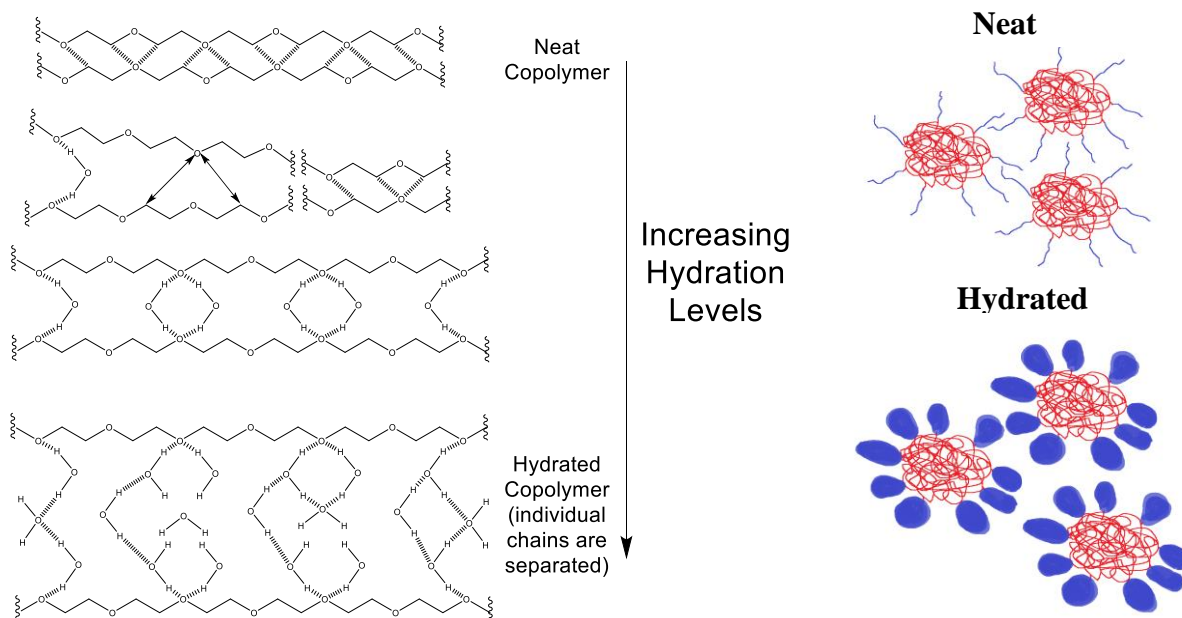


**Fig 3-6.** Effect of water content level on the PEG-PEG association of the block copolymers (left); differences in association between the neat copolymers (top) and hydrated copolymers (bottom).

Although the copolymers displayed changes in infinite shear viscosities with increasing hydration, the degree of change differed based on the wt% of PEG per

copolymer chain. The deviation in infinite shear viscosity observed in the materials with higher PEG wt % per copolymer chain was less than those with lower wt% PEG per copolymer chain (see Fig 3-3, ABA PEG 350–PDMS 17000 vs PEG 750–PDMS 17000 and BAB PEG 400–PDMS 850 vs PEG 1000–PDMS 850). As previously mentioned, the viscosity will continue to decrease until a threshold point is achieved where the hydrogen bonds being formed are able to overcome effects of the PEG-PEG dipole-dipole bonds being severed. As the PEG wt% per copolymer chain increases, greater wt% of water should also be needed to reach this threshold point. Consequentially, greater wt% of water should also be required to observe the increase in infinite shear viscosity for the materials with larger wt% PEG.

The infinite shear viscosities of the neat and hydrated copolymers with larger PDMS blocks (while the PEG block is kept constant) are higher than those with smaller PDMS blocks (see Fig 3-3, ABA PEG 350–PDMS 17000 vs PEG 350–PDMS 28000 and BAB PEG 400–PDMS 850 vs PEG 1000–PDMS 4750). This is likely due to the greater entanglements that are formed between the PDMS blocks of the copolymers leading to greater rigidity, which in turn leads to an increase in viscosity. It was also observed that the copolymers with larger PDMS blocks also display a lower degree of deviation in their infinite shear viscosities with increased hydration compared to copolymers with smaller PDMS chains. This phenomenon can also be correlated to the molecular entanglements formed between the PDMS blocks. Due to greater entanglements in the silicone block, the PEG will have a lower degree of flexibility as it is chemically tethered to the PDMS (see Fig 3-6). The lower flexibility of the overall copolymer should reduce the PEG's ability to be swollen (PEG blocks bound to each other via bridging hydrogen bonds), which occurs when the copolymer is hydrated. It is believed that there will be a lower

number of bridging interactions made between the PEG blocks due to the decrease in flexibility. These bridging interactions are required to see the changes in viscosity, thereby the copolymers with larger PDMS blocks will display a lower degree of deviation in infinite shear viscosity with changing hydration levels.

To further examine the effects of hydration on the PEG-PEG associations of the tri block copolymers, the infinite shear viscosities were plotted against water to PEG ratio (see Fig 3-7). The materials once again displayed a drop in viscosity followed by an increase in viscosity in a parabolic fashion. The drop in viscosity was seen to be occurring when the water to PEG ratio was lower than 0.2. This idea further validates the previous conclusions of hydration effecting the block associations and in turn the viscosity of the material.

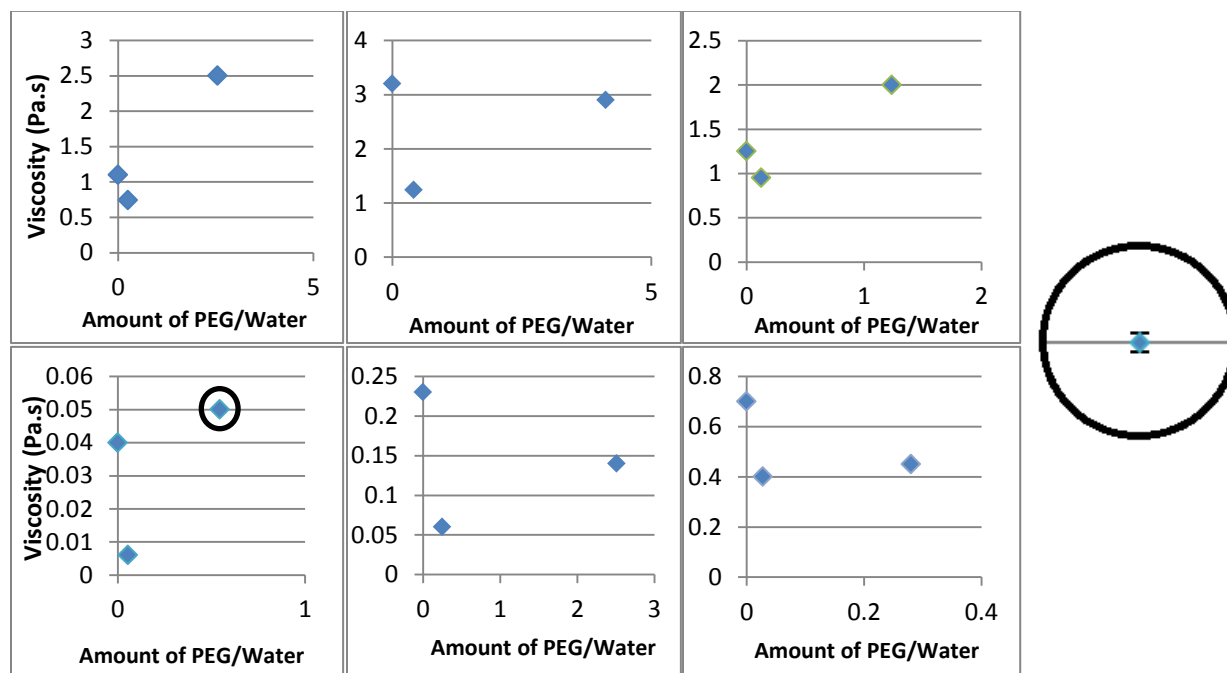


Fig 3-7. Infinite shear viscosities for the copolymers plotted against H<sub>2</sub>O:PEG ratio, row 1: ABA PEG 350-PDMS 17000 (left), ABA PEG 350-PDMS 28000 (middle), ABA PEG 750-PDMS 17000 (right); row 2: BAB PEG 400-PDMS 850 (left), BAB PEG 400-PDMS 4750 (middle), BAB PEG 1000-PDMS 850 (right); Enlarged picture of the data point with error which are in the 10<sup>-3</sup> scale (right).

### **3-4.2: Effect of PEG and PDMS composition per copolymer chain and molecular weight on the structural integrity**

Although the ABA and BAB materials exhibited shear thinning properties in their neat format, it was unknown if they would do so in the aqueous environment of the eye. It is well known that PEG has a propensity to adsorb significant amount of water via hydrogen bonds (able to accept two hydrogen bonds per oxygen atom) to create a hydration shell around itself.<sup>3</sup> It was observed that the copolymers with larger PEG compositions in both ABA and BAB format were better able to retain their structure when exposed to greater water contents. It is believed that the materials lost their structure when the PEG formed a significant number of hydrogen bonds with water (severing the PEG-PEG dipole bonds) to create a large hydration shell around itself, which eventually led to the separation of the individual chains from each other (see Fig 3-6). The PEG-PEG association in the copolymers with smaller PEG blocks are far weaker (due to a lower number of dipole-dipole interactions) than the copolymers with larger PEG blocks. Thus, copolymers with smaller PEG blocks will require a lower number of PEG-PEG dipole bonds broken (which would in turn require a lower degree of hydration) prior to the material losing its structure compared to the materials with larger PEG blocks.

Looking at the data more carefully, it was observed that the ABA copolymers created from 2000 g/mol PEG had a lower PEG composition ratio than the BAB copolymers made from 2000 g/mol PEG (see chapter 2, Table 2-4). Knowing this information, the BAB copolymers should be able to maintain its cohesive structure when exposed to greater water contents. However that was not the case, as it was observed that the BAB copolymers lost their structure when exposed to saturated aqueous



conditions, while the ABA copolymers did not. This idea leads us to believe that other forces must be in effect to ensure that the copolymers maintain their cohesive structures. This phenomenon can be attributed to the PDMS chain lengths. The PDMS chains on the BAB copolymers were significantly shorter (850 and 4750 g/mol) than those on the ABA copolymers (17000 and 28000 g/mol). In the hydrated systems, the PDMS blocks will collapse and aggregate with one another and form molecular entanglements. A longer chain will allow for a greater density of molecular entanglements (more difficult to separate the aggregate), thereby allowing the copolymers to retain its cohesive structure under more strenuous conditions (greater hydration to try and separate the individual copolymers). It is believed that due to the lower degree of molecular entanglements (between the PDMS blocks) in the BAB copolymers, the material loses its structure under a lower degree of hydration compared to the ABA copolymers which would form a more rigid aggregate structure.

### **3-4.3: Effect of PEG block size on light transmission of hydrated copolymers**

It was observed in our previous experiments that the materials with significant disparity in block composition were better able to transmit light compared to those with similar block ratios. Once the materials were hydrated, it was observed that the materials were able to transmit light based on the hydration level and the PEG:PDMS ratio. Maintaining the PDMS block size at 17000 or 28000 g/mol, it was observed that the copolymers with larger PEG block sizes (thereby higher PEG composition ratio) achieved optimal transparency at higher hydration levels (see Fig 3-4). However, after achieving the optimal transparency, the material becomes increasingly opaque as the water content was increased further. This is explained by the changes occurring in the refractive index of the PEG blocks with increasing hydration. It was observed that PEG

has a refractive index of  $\sim 1.46$  which slowly decreases as it is exposed to greater water content.<sup>6</sup> Furthermore, the results indicated that the refractive index of the materials exhibiting high light transmission is  $\sim 1.40$  (similar to silicone). Based on this, it can be speculated that the optimal transparency for the materials occur when the PEG is hydrated to a point where the refractive index is similar to that of silicone thus causing light to pass through the material without being reflected back: classical refractive index matching (see Fig 3-7).<sup>7</sup> However, with additional water the refractive index of the PEG continues to decrease, deviating from that of silicone, and the material becomes opaque. The materials with the larger PEG will require a larger amount of water to hydrate itself to reach a refractive index similar to silicone. That is why it is believed that the copolymers tethered to larger PEG blocks required greater water content to reach optimal transmission compared to their smaller counterparts.

The BAB copolymers displayed a similar trend where the copolymers with larger PEG chains required a greater degree hydration to achieve the optimal transmission level. Upon closer inspection it was also observed that when the PEG size was kept constant and the PDMS size was varied, the material with the larger PDMS chain achieved optimal transparency at a lower hydration level compared to its counterpart, which has a smaller PDMS chain tethered to it. This can also be explained with the PEG composition of the copolymer. Since the sample with the larger PDMS chain has a smaller PEG composition ratio, it would require less water to reach the required refractive index for optimal light transmission.

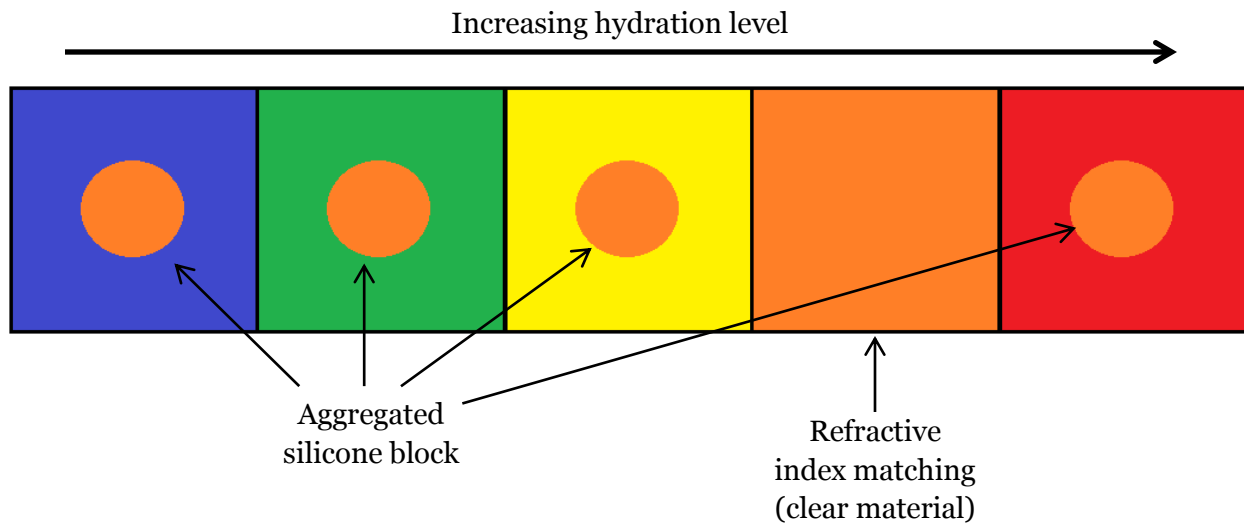


*Fig 3-8.* Effect of hydration on the refractive index of PEG.

### **3-4.4: Comparison of copolymers with past materials**

Previously, numerous copolymers were created using PEG for different purposes. It is widely used in the biomedical sector as it is non-immunogenic and hydrophilic.<sup>10-12</sup> PEG grafted onto dextran molecules have been tested for their shear thinning properties and it was observed that the materials required significant amount of time (several hours) to recover their original viscosities.<sup>13</sup> The recovery time for the copolymers created during this project (in both ABA and BAB format) was significantly faster (shear sweep tests were done in triplicates with 5 minute intervals, which revealed the same shear viscosity profiles for the material). In the case of a retinal tamponade, this would be helpful, as one would like a high viscosity material to form immediately after injection to ensure that there is no emulsification occurring.

Other triblock copolymers that have been used for retinal tamponades include pluronic F-127 (a poloxamer).<sup>9</sup> Although the material was optically clear and displayed shear thinning properties that would be useful in the injection procedure, it fell short due to toxic effects causing the surrounding cells to lyse.<sup>14</sup> The copolymers created in

this project are composed of two blocks (silicone and PEG) that have been thoroughly tested for their in-vivo effects and have been determined to be non-immunogenic and non-toxic.<sup>10-12,15-17</sup> Although, in-vitro and in-vivo toxicity tests were not performed on the copolymers, it is likely that since the individual blocks are highly biocompatible, the overall triblock copolymer should not pose a toxicity problem.

As previously mentioned, silicone oil is the current gold standard for retinal tamponades as they are highly biocompatible. Silicone oils are optically transparent and it remains that way when introduced into the aqueous environment of the eye.<sup>1</sup> However, they have a refractive index of  $\sim 1.404$  (significantly different from 1.33 refractive index of the natural vitreous), they pose the risk of glaucoma due to emulsification, and they do not completely fill the vitreous cavity to optimize the tamponade effect.<sup>18</sup> The ABA and BAB copolymers should be able to overcome emulsification problems of the silicone oil due to their high rest viscosities (which should reduce the emulsification process). Furthermore, the PEG molecules will introduce a hydrophilic characteristic to the copolymer which in turn should allow the material to better fill the vitreous cavity and thus act as a better retinal tamponade. However, these materials are opaque in nature unless the composition of one block is significantly higher than the other or they are exposed to a specific level of hydration to allow for refractive index matching. It is not possible to control the water content in the eye making these materials ineffective retinal tamponades.

### **3-4.5: Possible modifications to create an optimal retinal tamponade**

To create an optimal retinal tamponade, it should mimic the characteristics of the natural vitreous as closely as possible. The most important of these characteristics include, the ability to transmit light effectively, maintain a refractive index of  $\sim 1.33$

(refractive index of natural vitreous), and to ensure that the material does not emulsify to cause any blockages in the aqueous humor flow. An optimal retinal tamponade should be able to exude these characteristics in the aqueous environment of the eye. The data obtained from the experiments with the neat copolymers and the hydrated copolymers led to some interesting speculation. Both the ABA and BAB copolymers exhibit shear thinning properties when exposed to aqueous conditions. High rest viscosity for the materials should alleviate any emulsification problems, while the low shear viscosity should allow the materials to be injected in a cost effective manner. Furthermore, both the ABA and BAB the copolymers with larger PEG blocks are better able to retain their structure when exposed to higher levels of water. It was also observed that the ABA copolymers were better able to retain their cohesive structures when exposed to greater hydration levels due to their significantly large PDMS blocks. Seeing this, it is suggested that future PEG –PDMS copolymers made with the intention to act as retinal tamponade should be of ABA geometry. However, seeing as this material would force the user to utilize large PDMS blocks, it would defeat the purpose of creating a copolymer with a refractive index similar to that of the natural vitreous.

Alternatively, it may be better to create a material that utilizes a large PEG block (>2000 g/mol) tethered to a small PDMS block. As we have proven that this formulation works in the BAB format, it is suggested to follow this route since the PEG will then guide the overall refractive index of the copolymer. It has been shown that if there is a significantly large composition of one block, that block is essentially dictating the terms of the overall refractive index of the copolymer thus the material appears relatively clear. When the block compositions become more similar to one another, both refractive indices play a significant role, and thus can cause the material to be opaque.

Since we can effectively change the refractive index of the PEG block by changing the hydration levels, it may be possible to create a hydrated copolymer that has a refractive index that is closer to that of the natural vitreous. To do so, it may be possible to utilize a significantly large PEG block with very small PDMS blocks to create a significant disparity in the block composition ratios. Our research has proven that such copolymers should be shear thinning in nature and able to retain their shear thinning properties once hydrated. Due to the significantly large PEG block composition, PEG will dictate the overall refractive index and the PDMS block will have very little effect on the light transmission. Since, it was observed that copolymers with large PEG blocks are able to retain their cohesive structure under extreme hydration, it is possible to hydrate such copolymer significantly so that the refractive index becomes approximately 1.33.

Furthermore, it was observed that an ordered branched pendant group has the ability to act as a modifier to help increase the rest viscosity (if the central block is significantly large). This leads to believe that a triblock copolymer with small branched terminal ends would be more effective than linear terminal blocks, since higher viscosity materials should display a lower emulsification rate. Additionally, shear thinning behaviour was still observed with the small terminal branched blocks tethered to significantly large central blocks. The drop in viscosity was apparent at very low shear rates, which is promising. These observations will hopefully be helpful in the further development of new retinal tamponades.

Looking at the findings from this project, it is clear that it is very much possible to retain the structural integrity of the copolymers in a hydrated environment by adjusting the PEG:PDMS ratio of the copolymer chain. It is also possible to affect the light transmission capabilities of the copolymers by adjusting the hydration levels and

the copolymer composition to allow for the PEG and PDMS refractive index to be similar to one another. The parameters determined will act as guidelines for future research occurring on PEG-PDMS shear thinning copolymers that are to be used in an aqueous environment. This data will help narrow the selection of PEG:PDMS ratio to help create materials specific for the goals at hand.

### **3-5: Conclusion**

This work determined that PEG-PDMS copolymers of ABA and BAB geometry were able to retain their structural integrity and shear thinning properties in an aqueous environment provided that they retained their cohesive structure. The viscosities of the materials were adjusted by the hydration content due to the water effects on the PEG-PEG association. In both the ABA and BAB geometries, the PEG:PDMS composition ratio dictates if the material will retain its structural integrity and high viscosity in an aqueous environment. Materials with higher PEG composition ratio in both geometries were able to retain their structural integrity when exposed to greater water content. Furthermore, longer PDMS chains allow the copolymers to retain their cohesive structure when exposed to greater hydration due to greater molecular entanglements formed between the hydrophobic blocks. Lastly, materials with larger PEG composition ratios also require greater water content to achieve optical clarity to allow for high light transmission over the visible spectrum.

### **3-6: Acknowledgements**

I would like to thank Dr. Yang Chen for conducting the GPC tests. I would also like to thank the funding organizations: 20/20 ophthalmic network, OGS, and NSERC.

### **3-7: References**

1. Soman N, Banerjee R. Artificial vitreous replacements. *Bio-Medical Materials and Engineering*. 2003. 13: 59-74.
2. Chan YK, Cheung N, Chan WSC, Wong D. Quantifying silicone oil emulsification in patients: are we only seeing the tip of the iceberg? *Graefe's Archive for Clinical and Experimental Ophthalmology*. 2014.1-5.
3. Zolnik BS, Gonzalez-Fernandez A, Sadrieh N, Dobrovolskaia MA. Minireview: nanoparticles and the immune system. *Endocrinology*. 2010. 151(2):458-465.
4. Lewis LN, Stein J, Gao Y, Colborn RE, Hutchins G. Platinum catalysts used in the silicones industry. *Platinum Metals Review*. 1997. 41(2): 66-74.
5. Ottani S, Vitalini D, Comelli F, Castellari C. Densities, Viscosities, and Refractive Indices of Poly(ethylene glycol) 200 and 400 + Cyclic Ethers at 303.15 K. *Journal of Chemical Engineering*. 2002. 47(5): 1197-1204.
6. Mohsen-Nia M, Modarress H, Rasa H. Measurement and Modeling of Density, Kinematic Viscosity, and Refractive Index for Poly(ethylene Glycol) Aqueous Solution at Different Temperatures. *Journal of Chemical Engineering*. 2005. 50(5): 1662-1666.
7. Franklin J, Wang ZY. Refractive index matching: a general method for enhancing the optical clarity of a hydrogel matrix. *Chemistry of materials*. 2002. 14(11): 4487-4489.
8. Baino F. The Use of Polymers in the Treatment of Retinal Detachment: Current Trends and Future Perspectives. *Polymers*. 2010. 2: 286-322.
9. Baino F. Towards an Ideal biomaterials for vitreous replacement: Historical Overview and future trends. *Acta Biomaterialia*. 2011. 7(3): 921-935.
10. Sigma Aldrich. Poly(ethylene glycol) and Poly(ethylene oxide) [Internet]. 2014 [cited 2014 Nov 25]. Available from: <http://www.sigmaaldrich.com/materials-science/material-science-products.html?TablePage=20204110>
11. Harris JM, Chess RB. Effect of pegylation on pharmaceuticals. *Nature reviews: Drug discovery*. 2003. 2(3): 214-221.
12. Veronese FM, Pasut G. PEGylation, successful approach to drug delivery. *Drug discovery today*. 2005. 10(21): 1451-1458.
13. Guvendiren M, Lu HD, Burdick JA. Shear-thinning hydrogels for biomedical applications. *Soft Matter*. 2012. 8(2): 260-272.



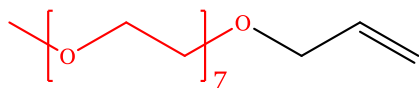
14. Davidorf F, Chambers RB, Kwon OW, Doyle W, Gresak P, Frank SG. Ocular toxicity of vitreal pluronic polyol F-127. *Retina*. 1990. 10(4): 297-300.
15. Lloyd AW, Faragher RGA, Denyer SP. Ocular biomaterials and implants. *Biomaterials*. 2001. 22(8): 769-785.
16. François B, Colas A, Thomas X. Silicones for medical use. In XIIIth Technical Congress: Polymers for Biomedical Use. 1996.
17. Abbasi F, Mirzadeh H, Katbab AA. Modification of polysiloxane polymers for biomedical applications: a review. *Polymer International*. 2001. 50(12): 1279-1287.
18. Colthurst MJ, Williams RL, Hiscott PS, Grierson I. Biomaterials used in the posterior segment of the eye. *Biomaterials*. 2000. 21(7): 649-665.

## **Appendix A:**

### **A-1: Chemical structures and <sup>1</sup>H-NMR of allylated PEG**

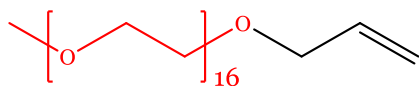
#### **A-1.1: Monoallylated PEG**

350 g/mol PEG



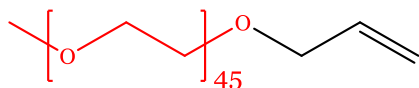
<sup>1</sup>H NMR (CDCl<sub>3</sub>): δ = 3.28 (s, 3H); 3.44-3.63 (m, 28H); 3.94 (dt, 2H); 5.06-5.21 (m, 2H); 5.83 (m, 1H).

750 g/mol PEG



<sup>1</sup>H NMR (CDCl<sub>3</sub>): δ = 3.34 (s, 3H); 3.48-3.74 (m, 64H); 3.98 (dt, 2H); 5.11-5.26 (m, 2H); 5.87 (m, 1H).

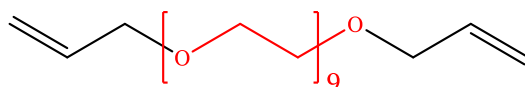
2000 g/mol PEG



<sup>1</sup>H NMR (CDCl<sub>3</sub>): δ = 3.37 (s, 3H); 3.50-3.76 (m, 190H); 4.01 (dt, 2H); 5.15-5.29 (m, 2H); 5.90 (m, 1H).

#### **A-1.2: Diallylated PEG**

400 g/mol PEG



<sup>1</sup>H NMR (CDCl<sub>3</sub>): δ = 3.55-3.71 (m, 36H); 3.99 (dt, 4H); 5.12-5.28 (m, 4H); 5.88 (m, 2H).

1000 g/mol PEG



$^1\text{H NMR}$  ( $\text{CDCl}_3$ ):  $\delta = 3.51\text{-}3.79$  (m, 88H); 4.02 (dt, 4H); 5.15-5.30 (m, 4H); 5.91 (m, 2H).

2000 g/mol PEG

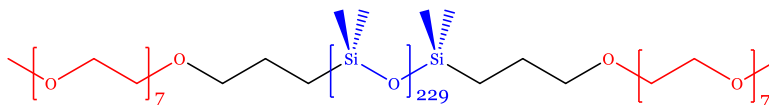


$^1\text{H NMR}$  ( $\text{CDCl}_3$ ):  $\delta = 3.51\text{-}3.81$  (m, 36H); 4.02 (dt, 4H); 5.15-5.31 (m, 4H); 5.91 (m, 2H).

## **A-2: Chemical structures and H NMR of linear ABA and BAB block copolymers**

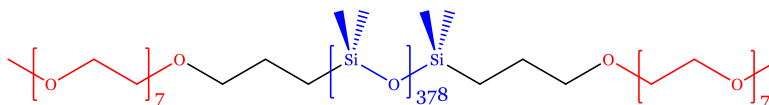
### A-2.1: Linear ABA Block copolymers

350 g/mol PEG – 17000 g/mol PDMS



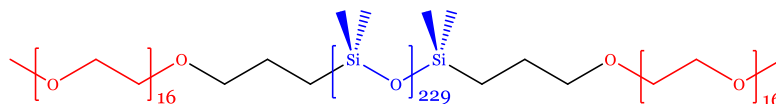
$^1\text{H NMR}$  ( $\text{CDCl}_3$ ):  $\delta = 0.08$  (m, 1380H); 0.52 (t, 4H); 1.62 (t, 4H); 3.39 (s, 6H); 3.42 (t, 4H); 3.53-3.70 (m, 56H).

350 g/mol PEG – 28000 g/mol PDMS



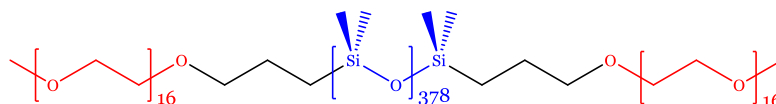
$^1\text{H NMR}$  ( $\text{CDCl}_3$ ):  $\delta = 0.09$  (m, 2274H); 0.52 (t, 4H); 1.62 (t, 4H); 3.39 (s, 6H); 3.43 (t, 4H); 3.53-3.72 (m, 56H).

750 g/mol PEG – 17000 g/mol PDMS



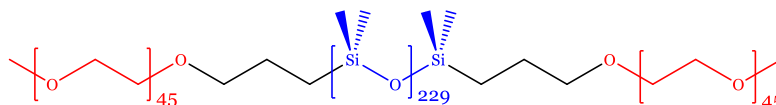
<sup>1</sup>H NMR (CDCl<sub>3</sub>): δ = 0.09 (m, 1380H); 0.53 (t, 4H); 1.63 (t, 4H); 3.39 (s, 6H); 3.43 (t, 4H); 3.53-3.71 (m, 128H).

750 g/mol PEG – 28000 g/mol PDMS



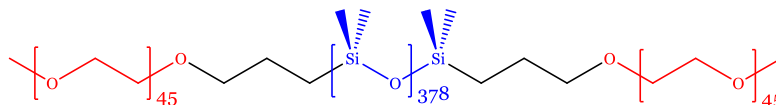
<sup>1</sup>H NMR (CDCl<sub>3</sub>): δ = 0.09 (m, 2274H); 0.53 (t, 4H); 1.62 (t, 4H); 3.39 (s, 6H); 3.42 (t, 4H); 3.55-3.71 (m, 128H).

2000 g/mol PEG – 17000 g/mol PDMS



<sup>1</sup>H NMR (CDCl<sub>3</sub>): δ = 0.08 (m, 1380H); 0.53 (t, 4H); 1.60 (t, 4H); 3.39 (s, 6H); 3.42 (t, 4H); 3.52-3.70 (m, 180H).

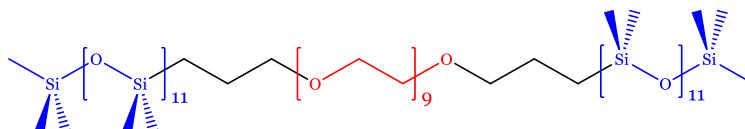
2000 g/mol PEG – 28000 g/mol PDMS



<sup>1</sup>H NMR (CDCl<sub>3</sub>): δ = 0.08 (m, 2274H); 0.53 (t, 4H); 1.63 (t, 4H); 3.39 (s, 6H); 3.42 (t, 4H); 3.52-3.72 (m, 180H).

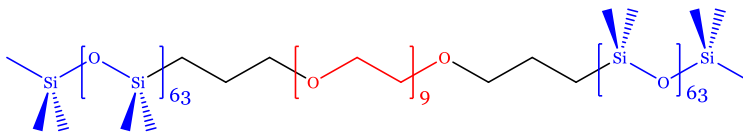
### A-2.2: Linear BAB Block copolymers

400 g/mol PEG – 850 g/mol PDMS



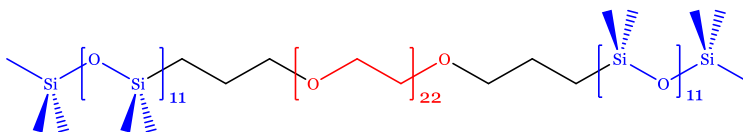
$^1\text{H}$  NMR ( $\text{CDCl}_3$ ):  $\delta = 0.08$  (m, 150H); 0.54 (t, 4H); 1.62 (t, 4H); 3.42 (t, 4H); 3.57-3.75 (m, 36H).

400 g/mol PEG – 4750 g/mol PDMS



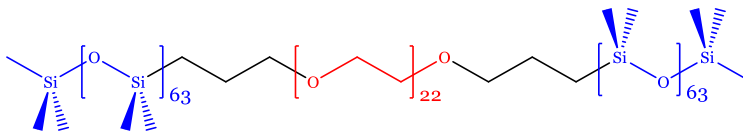
$^1\text{H}$  NMR ( $\text{CDCl}_3$ ):  $\delta = 0.08$  (m, 774H); 0.54 (t, 4H); 1.62 (t, 4H); 3.42 (t, 4H); 3.58-3.80 (m, 36H).

1000 g/mol PEG – 850 g/mol PDMS



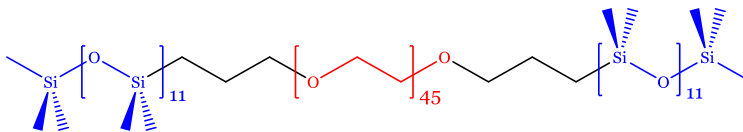
$^1\text{H}$  NMR ( $\text{CDCl}_3$ ):  $\delta = 0.08$  (m, 150H); 0.54 (t, 4H); 1.62 (t, 4H); 3.42 (t, 4H); 3.51-3.79 (m, 48H).

1000 g/mol PEG – 4750 g/mol PDMS



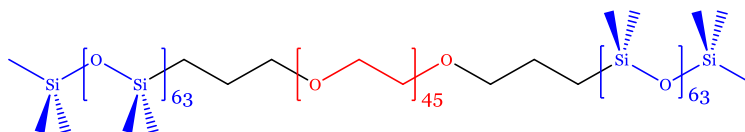
$^1\text{H}$  NMR ( $\text{CDCl}_3$ ):  $\delta = 0.08$  (m, 774H); 0.54 (t, 4H); 1.62 (t, 4H); 3.42 (t, 4H); 3.52-3.80 (m, 48H).

2000 g/mol PEG – 850 g/mol PDMS



$^1\text{H}$  NMR ( $\text{CDCl}_3$ ):  $\delta = 0.08$  (m, 150H); 0.54 (t, 4H); 1.61 (t, 4H); 3.42 (t, 4H); 3.50-3.79 (m, 180H).

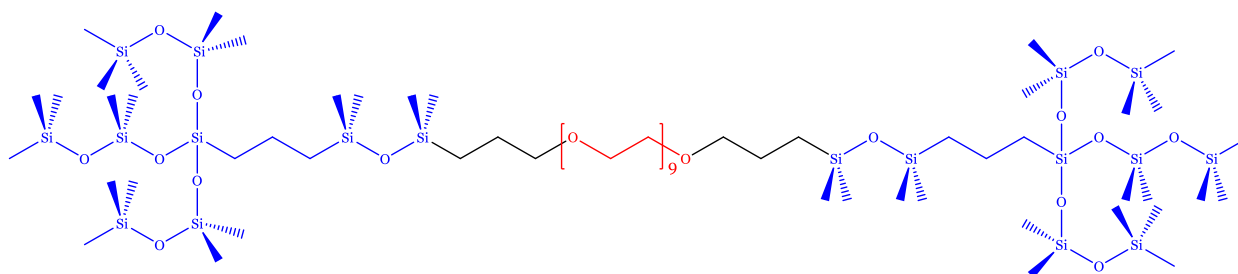
2000 g/mol PEG – 4750 g/mol PDMS



$^1\text{H}$  NMR ( $\text{CDCl}_3$ ):  $\delta = 0.08$  (m, 774H); 0.54 (t, 4H); 1.62 (t, 4H); 3.42 (t, 4H); 3.52-3.80 (m, 180H).

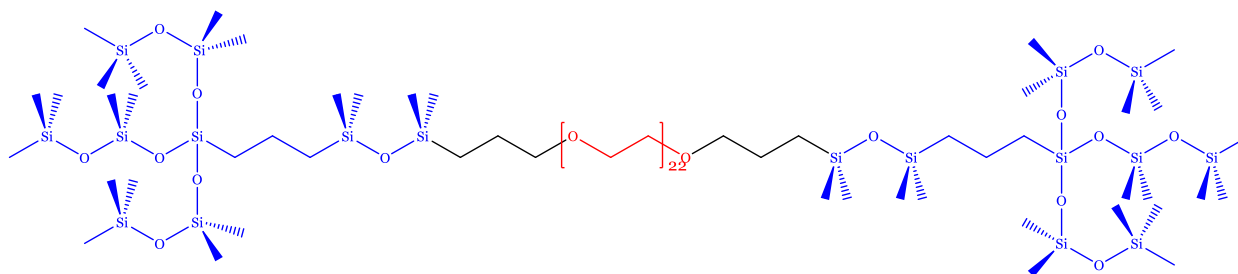
### A-3: Chemical structures and H NMR of $^b\text{BA}^b\text{B}$ block copolymers

400 g/mol PEG – 692 g/mol branched pendant group



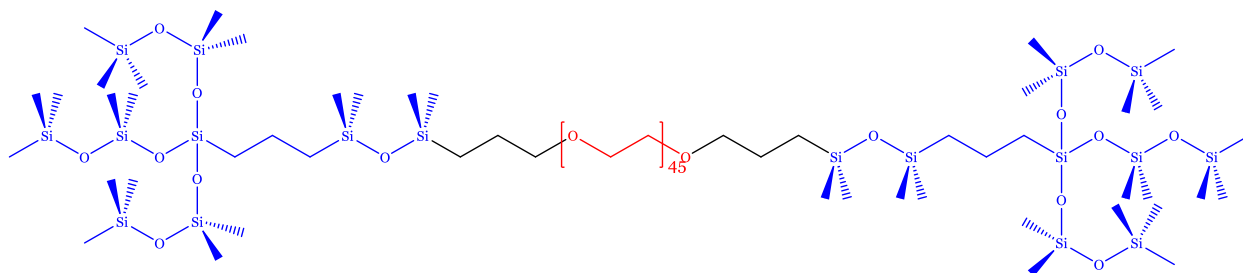
$^1\text{H}$  NMR ( $\text{CDCl}_3$ ):  $\delta = 0.05$  (m, 36H); 0.08 (m, 78H); 0.55-0.61 (m, 12H); 1.37-1.48 (m, 8H); 3.41 (t, 4H); 3.50-3.80 (m, 36H).

1000 g/mol PEG – 692 g/mol branched pendant group



$^1\text{H}$  NMR ( $\text{CDCl}_3$ ):  $\delta = 0.04$  (m, 36H); 0.07 (m, 78H); 0.54-0.60 (m, 12H); 1.37-1.47 (m, 8H); 3.39 (t, 4H); 3.50-3.79 (m, 88H).

2000 g/mol PEG – 692 g/mol branched pendant group



$^1\text{H NMR}$  ( $\text{CDCl}_3$ ):  $\delta = 0.03$  (m, 36H); 0.06 (m, 78H); 0.53-0.59 (m, 12H); 1.36-1.44 (m, 8H); 3.39 (t, 4H); 3.48-3.77 (m, 180H).